

REVIEW ARTICLE

Open Access



A review of advanced architectural glazing technologies for solar energy conversion and intelligent daylighting control

Xiao Liu and Yupeng Wu*

Abstract

Efficient management of solar radiation through architectural glazing is a key strategy for achieving a comfortable indoor environment with minimum energy consumption. Conventional glazing consisting of a single or multiple glass pane(s) exhibits high visible light transmittance and solar heat gain coefficient, which can be a double-edged sword, i.e., it allows sufficient sunlight to enter the building interior space for passive heating and lighting; on the other hand, it can cause glare discomfort and large cooling energy consumption. Among the various advanced glazing technologies being developed, Building Integrated Photovoltaic (BIPV) glazing has a prominent position due to its ability to reduce cooling load and visual discomfort while simultaneously generating electricity from sunlight. Recent years have witnessed remarkable advances in low-concentration optics such as Dielectric based Compound Parabolic Concentrators (DiCPCs), with a growing interest in the development of Building Integrated Concentrating Photovoltaic (BICPV) glazing to improve light harvesting and electric power output. One of the challenges faced by traditional BIPV glazing systems is the lack of dynamic control over daylight and solar heat transmission to cope with variations in weather conditions and seasonal heating/cooling demands of buildings. A promising solution is to integrate an optically switchable smart material into a BIPV glazing system, which enables dynamic daylighting control in addition to solar power conversion. Thermotropic (TT) hydrogel materials such as poly(N-isopropylacrylamide) (PNIPAm) and Hydroxypropyl Cellulose (HPC) are potential candidates for hybrid BIPV smart glazing applications, due to their unique features such as high visible transparency (in the clear state), strong light-scattering capability (in the translucent state) and large solar energy modulation. This paper reviews various types of electricity-generating glazing technologies including BIPV glazing and BICPV glazing, as well as smart glazing technologies with a particular focus on TT hydrogel integrated glazing. The characteristics, benefits and limitations of hybrid BIPV smart glazing are also evaluated. Finally, the challenges and research opportunities in this emerging field are discussed.

Keywords: Photovoltaic (PV), Solar concentrator, Smart glazing, Thermotropic hydrogel, Energy saving, Visual comfort

1 Introduction

With a growing concern about climate change, efforts to reduce fossil fuel consumption and greenhouse gas emissions are being made in various fields. The building sector is one of the leading energy consumers and carbon dioxide

emitters of the world (Skandalos & Karamanis, 2015). The energy used by residential and commercial buildings in developed countries represents 20–40% of the total energy consumption, and around 60% of all energy in buildings is consumed for space heating, space cooling, ventilation and electric lighting (Gorgolis & Karamanis, 2016; Hee et al., 2015; Kamalisarvestani et al., 2013; Rezaei et al., 2017). Energy conservation and on-site renewable energy production are two main strategies required to be adopted in

*Correspondence: Yupeng.Wu@nottingham.ac.uk

Department of Architecture and Built Environment, Faculty of Engineering,
The University of Nottingham, University Park, Nottingham NG7 2RD, UK

the design and operation of buildings, particularly when considering the urgent need in many developed countries for the transition towards near Zero Energy Buildings (n-ZEBs) (Favoino et al., 2015).

Windows are an essential part of buildings, providing access to light, heat, vision, sound and fresh air, and directly related to the comfort and health of occupants (Rezaei et al., 2017). Among the functionalities offered by windows, solar heat gain and visible light transmission represent two vital factors in the energy and environmental performance of buildings. Solar Heat Gain Coefficient (SHGC) is a measure of how much solar energy passes through a window, expressed by a ratio in the range of 0 to 1. Figure 1 (a) illustrates an example of solar heat transfer through a traditional single-glass window. The window has a SHGC of 0.86, which equals the solar transmittance (83%) of the glass plus the glass absorbed heat that is re-radiated to the indoor space (3%). The transmittance of a single clear glass in the visible range (380–780 nm) is approximately 90%, as illustrated in Fig. 1 (b). Traditional windows with both high SHGC and visible light transmittance (τ_{vis}) are often the reasons for overheating and glare issues (Tällberg et al., 2019). Employing solar shading devices such as curtains and blinds can block solar heat and glare from windows, however, at the expense of useful daylight so that electric lighting has to be operated in indoor

spaces despite high external light availability (Piccolo & Simone, 2015).

In this picture, a critical step is to minimise the quantities of unwanted solar heat and daylight through windows that account for substantial building energy consumption and occupant discomfort. Two approaches can be considered to improve window performance:

- (1) Integrating windows with light-absorbing materials/devices (e.g., photovoltaics, solar thermal collectors, phase change materials) to convert incident solar energy into electrical energy, thermal energy, chemical energy, etc.
- (2) Embedding optically switchable materials (e.g., thermotropic materials and electrochromic materials) in windows to intelligently regulate solar heat gain and daylighting in accordance with climatic conditions or user demands.

Within this work, a review is given on the recent development of advanced glazing technologies with either or both functions of electricity generation and intelligent daylighting control. This review aims to open a new route to improve the performance of current glazing technologies, for instance, to achieve higher electricity output of BIPV glazing and stronger solar

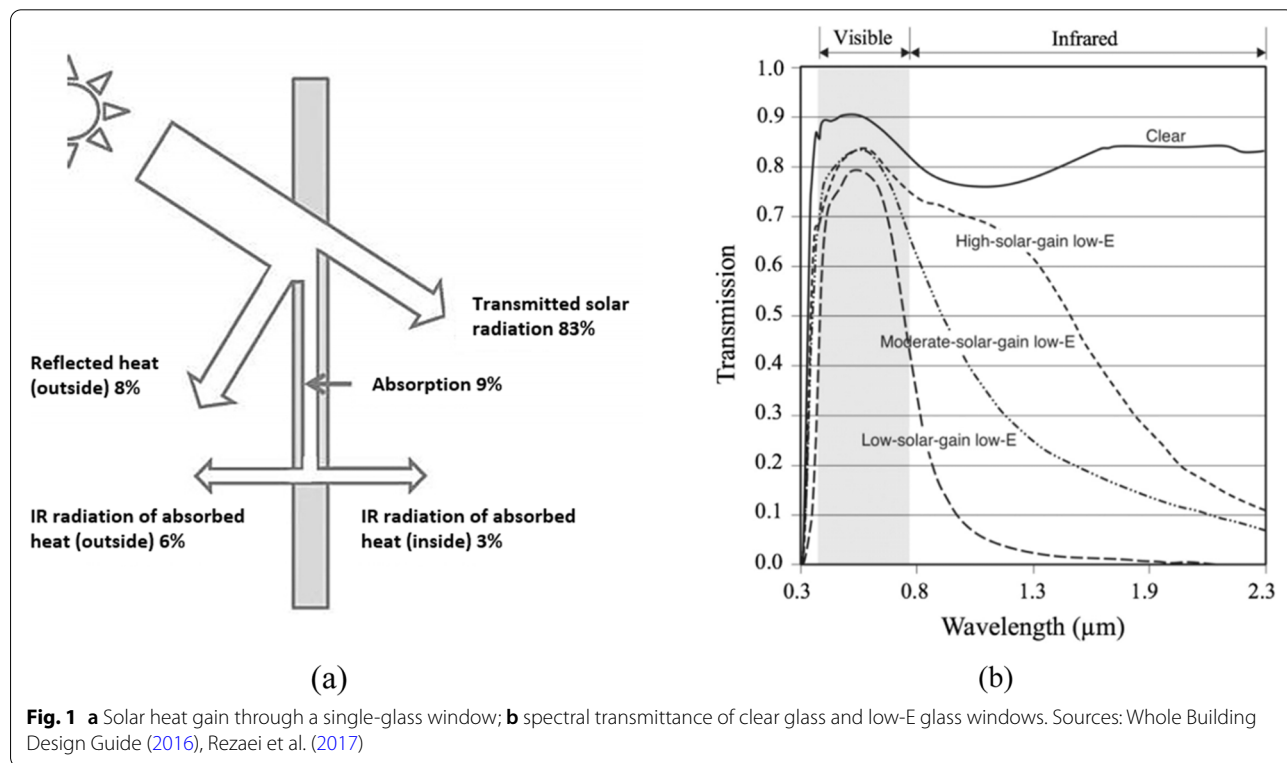


Fig. 1 a Solar heat gain through a single-glass window; b spectral transmittance of clear glass and low-E glass windows. Sources: Whole Building Design Guide (2016), Rezaei et al. (2017)

modulation ability of smart glazing. To do this, the paper is structured in the following five sections:

Section 2 - an overview of presently available glazing technologies.

Section 3 - an in-depth review of BIPV glazing and Concentrating PV (CPV) systems.

Section 4 - a systematic review of thermotropic hydrogel based smart windows.

Section 5 - a brief review of switchable PV glazing systems.

Section 6 - a discussion of the pros and cons of each glazing technology. Directions for future research are discussed as well.

2 Overview of traditional and advanced glazing technologies

Traditional windows are typically constituted of a single or double pane(s) of clear float glass with high τ_{vis} (>0.8) and SHGC (>0.7) (Casini, 2016; Rezaei et al., 2017) (see Fig. 2). Both values could be reduced if changing the clear glass to body-tinted glass, also known as absorptive

glass (Leftheriotis & Yianoulis, 2012). Tinted glass blocks light transmission through bulk absorption and re-emits a portion of the absorbed heat indoors as it warms up. Such glazing allows a great reduction in τ_{vis} but yields a modest reduction in SHGC (Leftheriotis & Yianoulis, 2012). Reflective glass is glass that has been treated with a metallic or metallic oxide coating, exceptional at rejecting glare and solar heat due to broadband high reflectance (Aguilar et al., 2015; Cuce & Riffat, 2015; Rezaei et al., 2017). The SHGC depends on the coating's thickness, reflectivity and location on the glass pane (Chow et al., 2010). However, reflective glass has a mirror-like appearance, which may cause disturbances on traffic roads and neighbour buildings but also obstruct the visual access to the indoors and outdoors (Chow et al., 2010). Float glass coated with a spectrally selective coating, such as low-emissivity (low-E) coating, can reduce unwanted heat exchange between the indoor and outdoor environments by reflecting infrared radiation while preserving high visible transparency. Low-E glass windows can be formulated with a broad range of SHGCs (see Fig. 1 (b)) to balance the demands of thermal insulation, solar heat gain and daylighting (Jelle et al., 2015; Rezaei et al., 2017).

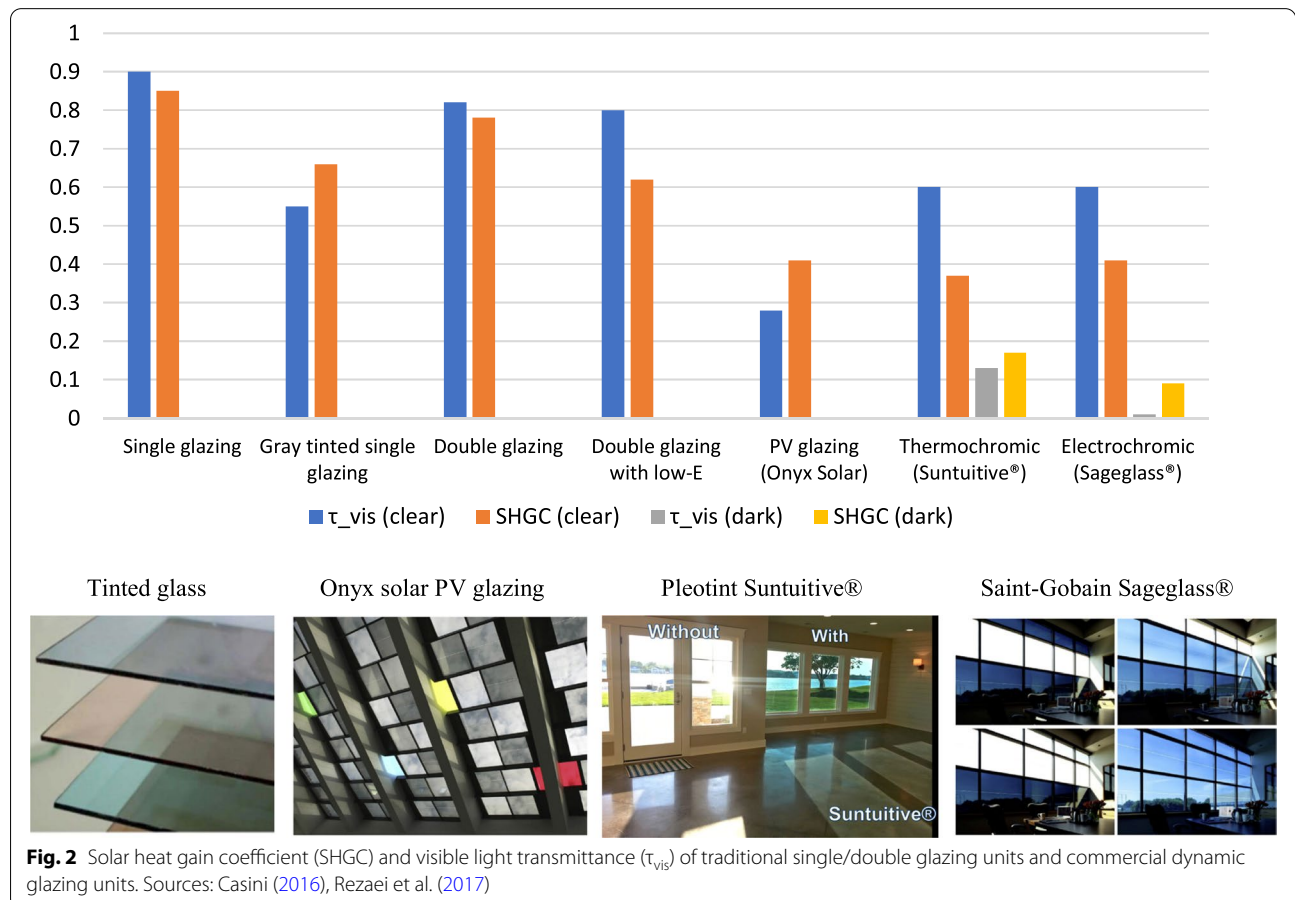


Fig. 2 Solar heat gain coefficient (SHGC) and visible light transmittance (τ_{vis}) of traditional single/double glazing units and commercial dynamic glazing units. Sources: Casini (2016), Rezaei et al. (2017)

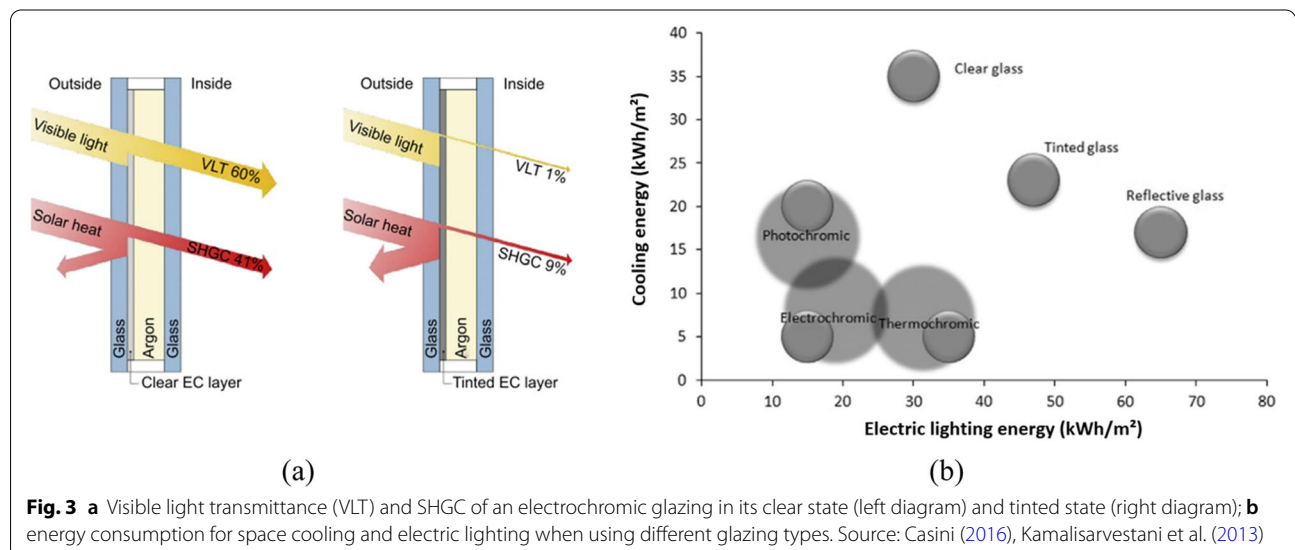
For example, the commercial low-E glazing products, Climaguard 80/70 with τ_{vis} of 0.8 and a high SHGC of 0.7 is intended for promoting window solar heat gain in heating-dominated climates, while Climaguard 70/36 with τ_{vis} of 0.7 and a low SHGC of 0.36 is intended for suppressing window solar heat gain in cooling-dominated climates (Jelle et al., 2015). Apart from using low-E coating, the thermal insulation of a window can be enhanced by increasing the number of glass panes, optimising the air layer thickness, and filling the cavity between glass panes with inert gas such as argon, krypton or xenon (Arıcı et al., 2015; Arıcı & Kan, 2015; Karabay & Arıcı, 2012). For instance, replacing a double-pane glazing with a triple or quadruple-pane glazing can reduce the heat loss by approximately 50% or 67% (Arıcı et al., 2015).

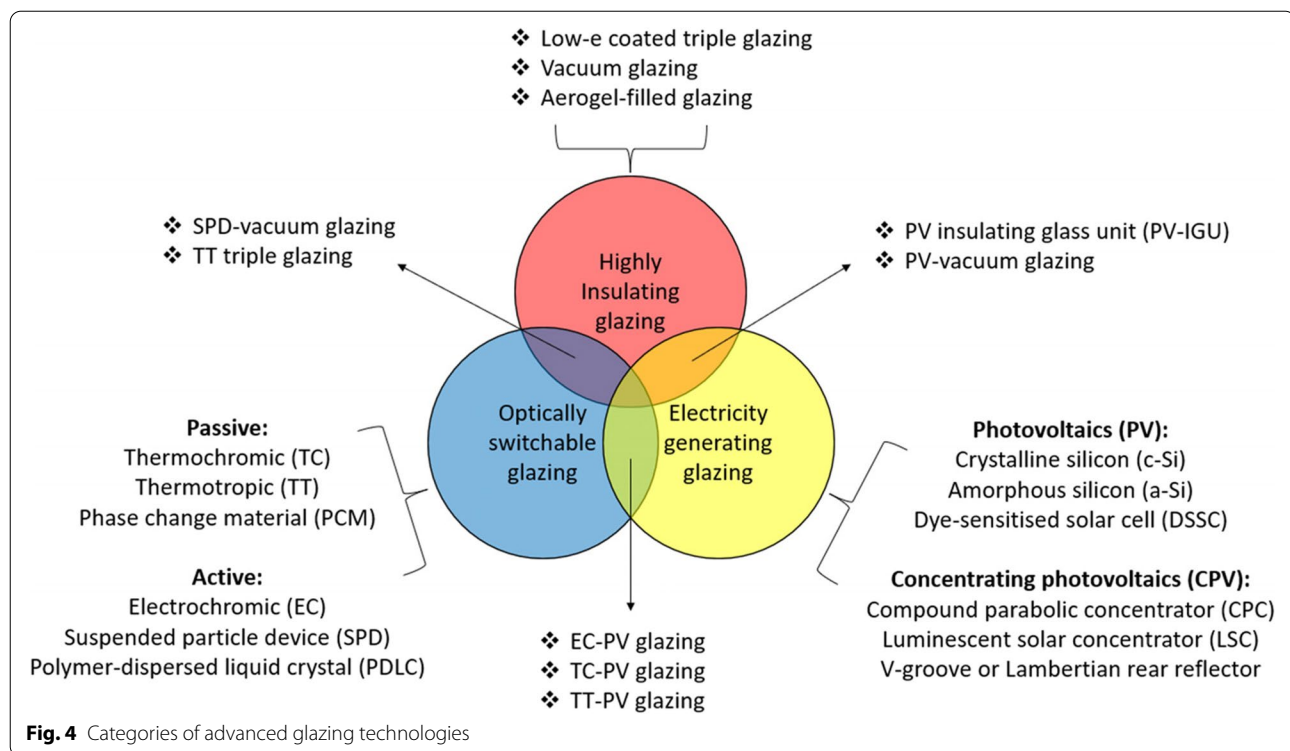
In continuous efforts to improve window performance, a variety of solar energy materials have been proposed for window integration, such as photovoltaic (PV) cells (Skandalos & Karamanis, 2015) and optically switchable smart materials (Casini, 2018). Window integrated photovoltaics can convert a fraction of the absorbed solar energy into usable electrical power instead of re-emitting it indoors, hence offering a more efficient way to reduce SHGC in comparison to tinted glass windows. For example, Onyx solar supplies a series of amorphous silicon (a-Si) thin-film PV glazing with SHGC (τ_{vis}) ranging from 0.22 (0.2%) to 0.41 (28.4%) (Casini, 2016). One challenge that PV glazing technologies have faced is simultaneous optimisation of visible light transmittance and Power Conversion Efficiency (PCE) (Hee et al., 2015; Peng et al., 2019). Because PV cells utilise visible radiation to produce electricity, on a technical level, it is not feasible to manufacture a PV glazing unit with both high PCE and

τ_{vis} (Casini, 2016; Peng et al., 2019; Skandalos & Karamanis, 2015). For economic reasons, commercial PV glazing products are typically manufactured with low τ_{vis} (below 30%) in order to achieve a reasonable PCE (Casini, 2016; Husain et al., 2018). For building applications, using PV glazing with low τ_{vis} and SHGC can alleviate the issues of glare and thermal discomfort to occupants, but also reduce the energy consumption for space cooling. Conversely, it would increase the heating load as well as the electric lighting load (to maintain desired indoor illuminance levels).

Windows integrated with smart materials such as thermochromic materials (Kamalisarvestani et al., 2013), photochromic materials (Wu et al., 2017) or electrochromic materials (Baetens et al., 2010) can alter their SHGC and τ_{vis} in response to an external stimulus such as temperature, light intensity or voltage. For example, an electrochromic window offers lower values of SHGC and τ_{vis} when switching from a clear state to a tinted state, as can be seen from Fig. 3 (a). In terms of energy saving, using an electrochromic window can potentially achieve lower energy demands for cooling and electric lighting than using traditional windows based on clear, tinted and reflective glass, as shown in Fig. 3 (b).

Presently available glazing technologies typically fall into three categories: highly insulating glazing, electricity-generating glazing and optically switchable (or smart) glazing (see Fig. 4). In recent years, multi-functional hybrid glazing has emerged as a promising candidate for the next generation of energy-efficient glazing technologies. For example, PV glazing can be combined with highly insulated glazing such as vacuum glazing to reduce heat loss (Ghosh & Norton, 2018; Radwan





et al., 2020). PV glazing can also be combined with smart glazing such as electrochromic (EC) glazing to form photovoltachromic glazing (or called self-powered switchable glazing) to adapt with diurnal variation of weather and thus improve the control of solar heat gain and daylighting in buildings (Favoio et al., 2016; Ghosh & Norton, 2018). It is also feasible to develop low-heat-loss switchable glazing systems such as EC-vacuum glazing and Suspended-Particle-Device (SPD)-vacuum glazing (Ghosh et al., 2017; Ghosh & Norton, 2018). The following sections provide a review of existing advanced glazing technologies, with a particular focus on PV glazing, CPV glazing, thermotropic smart glazing and switchable PV glazing.

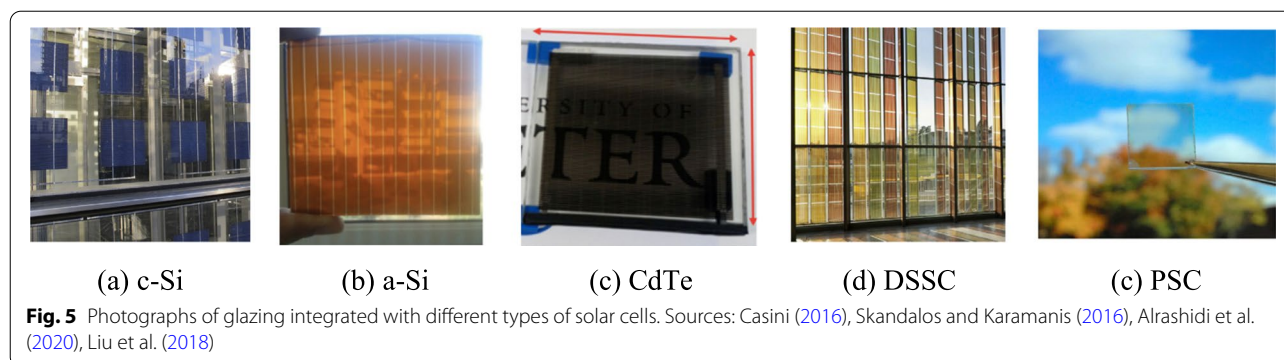
3 Electricity generating glazing technologies

Photovoltaic devices can absorb incident solar radiation and convert it into electricity. Building Integrated PV (BIPV) glazing is among the most promising solutions for n-ZEB design, due to utilisation of solar energy for producing electricity on site as well as reduction of cooling load and visual discomfort. Building Integrated Concentrating PV (BICPV) glazing is a key development in moving BIPV glazing towards higher electricity-generation potentials. The characteristics of BIPV and BICPV glazing technologies are described in Section 3.1 and Section 3.2, respectively.

3.1 Building integrated photovoltaic glazing

BIPV glazing can be produced by integrating solar cells into architectural glazing. Figure 5 shows examples of glazing integrated solar cells, including crystalline silicon (c-Si) solar cell and four different thin-film solar cells which are amorphous silicon (a-Si) solar cell, Cadmium Telluride (CdTe) solar cell, Dye-Sensitised Solar Cell (DSSC) and Perovskite Solar Cell (PSC). BIPV glazing has many benefits such as on-site electricity generation, reduction of solar heat gain and glare, energy saving and architectural elegance. These benefits have been verified through numerical and experimental investigations (see Table 1).

Crystalline silicon (c-Si) solar cells are a well-established technology with a few advantages such as high PCE and long-term operational stability (Cannavale, Hörantner, et al., 2017; Cannavale, Ierardi, et al., 2017; Ghosh et al., 2019; Skandalos & Karamanis, 2015). The typical efficiencies of monocrystalline silicon (mono-Si) solar cells and polycrystalline silicon (poly-Si) solar cells are 16–24% and 14–18%, respectively (Jelle et al., 2012; Skandalos & Karamanis, 2015). In general, c-Si BIPV glazing is manufactured through encapsulating an array of opaque c-Si solar cells between two panes of glass by using ethylene-vinyl acetate (EVA) films or optically clear bonding materials (e.g., polyvinyl butyral (PVB) and silicone resin) (Casini, 2016; Skandalos & Karamanis, 2015). Varying degrees of transparency of c-Si BIPV glazing



can be achieved by changing the PV cell coverage ratio, i.e., the fraction of the glazing aperture area covered by solar cells. In other words, the higher PV cell coverage ratio (or the shorter distance between adjacent c-Si cells), the lower glazing transparency. A higher PV cell coverage ratio is generally associated with a lower SHGC and higher electric power output. However, this would negatively impact the indoor daylight level, the use of electric lighting and the satisfaction of occupants with the amount of outside view (Skandalos & Karamanis, 2015).

Xu et al. (2014) simulated the building energy performance of c-Si BIPV windows in central China by using EnergyPlus. The optimal PV cell coverage ratio for achieving the lowest overall energy consumption was determined for a different combination of architectural variables, including window orientation and Window-to-Wall Ratio (WWR) (see Fig. 6). Chen et al. (2019) evaluated the energy-saving potential of c-Si BIPV windows under various climatic conditions in southwest China through EnergyPlus simulation and field measurement. It was found that a maximum of 83% reduction in annual energy consumption was achieved by using the optimised BIPV window (i.e., PV cell coverage ratio of 0.87, WWR of 0.83 and south orientation), compared to an ordinary double-glazed window.

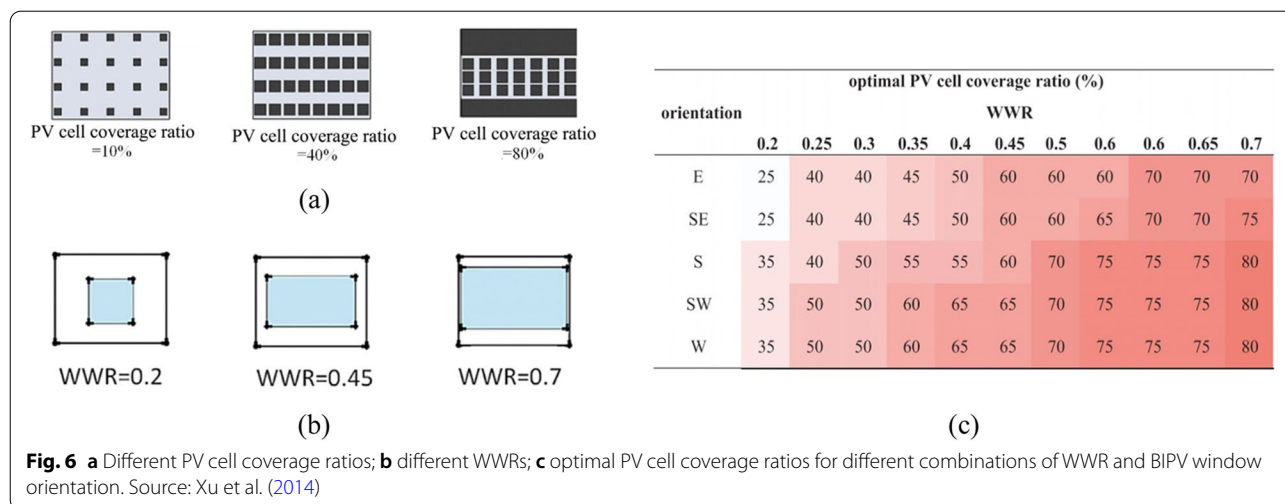
Thin-film solar cells, which are semi-transparent, uniform in appearance, flexible and lightweight, are of particular interest for BIPV glazing applications. Unlike c-Si solar cells with a thickness of up to 200 μm , thin-film solar cells have a thickness of the order of a few microns (Andreani et al., 2019). Thin-film manufacturing techniques such as Plasma-Enhanced Chemical Vapour Deposition (PECVD) allow thin films of varying thickness to be deposited on transparent substrates such as glass and plastic (Chae et al., 2014; Gao et al., 2017). For enhanced transparency, thin-film solar cell layers can be either made extremely thin or patterned by laser cutting (Liao & Xu, 2015; Meillaud et al., 2015; Peng et al., 2019). Amorphous silicon (a-Si) solar cell is

a well-developed thin-film PV technology (Skandalos & Karamanis, 2015). Due to the thinner layer produced, an a-Si solar cell requires less amount of silicon for its manufacture and thus costs less compared to a c-Si solar cell. Moreover, a-Si solar cells are less affected than c-Si solar cells by high operating temperature, shading and air pollution, allowing greater flexibility in building integration (Casini, 2016; Ogbomo et al., 2017). Although many efforts such as surface texturisation and adding anti-reflection coatings have been made to enhance the optical absorption of a-Si solar cells, the power conversion efficiency can hardly exceed 12% (Chae et al., 2014; Luceño-Sánchez et al., 2019; Meillaud et al., 2015).

Cadmium Telluride (CdTe) solar cells are well suited for BIPV glazing applications with cost and performance advantages over a-Si solar cells. The record laboratory efficiency of CdTe solar cells is 22.1% by First Solar (National Renewable Energy Laboratory, 2022). In addition, CdTe can be deposited onto large-area substrates more easily and faster when compared with a-Si (Alrashidi et al., 2019; Ogbomo et al., 2017). So far, CdTe is one of the few thin-film materials to compete with c-Si in terms of cost per watt (Ogbomo et al., 2017). On the other hand, CdTe is a potentially toxic material and could pose some adverse effects on the ecological environment and human health. Sun et al. (2018) demonstrated the effect of a commercial CdTe glazing product with 10% transparency on building energy performance by EnergyPlus simulation. Taking the case of an office building with a WWR of 75% in Beijing's climate as an example, the result shows that replacing 80% of the clear-glass window area by the CdTe glazing can achieve a 67.9% reduction in annual total energy consumption. Liu et al. (2020) explored the effect of CdTe windows on the visual comfort of occupants through a holistic consideration of transmitted daylight quantity and quality by RADIANCE simulation. Figure 7 shows the predicted values of UDI, DGP, CCT and CRI for CdTe windows with different degrees of visual transparency when applied to a cellular

Table 1 Studies on BIPV glazing technologies

Ref	Type	Objective	Method	Region	Major outcome
Fung and Yang (2008)	c-Si	To develop a 1D transient heat transfer model	EnergyPlus simulation	Hong Kong (China)	About 70% reduction in total heat gain for a PV cell coverage ratio of 0.8
Park et al. (2010)	c-Si	To assess the temperature effect on the electrical performance of a BIPV façade module	Indoor & Outdoor experiments	South Korea	0.52% reduction in power output per 1 °C increase in the module's temperature
Miyazaki et al. (2005)	a-Si	To find the optimal solar cell transmittance and WWR for a semi-transparent BIPV	EnergyPlus simulation	Tokyo (Japan)	Largest energy saving potential for 50% WWR and 40% solar cell transmittance
Wang et al. (2016)	a-Si	To investigate the energy-saving potential of a semi-transparent PV insulating unit	EnergyPlus simulation	Hong Kong (China)	25.3% reduction in annual energy usage compared to a clear single-glass window
Peng et al. (2016)	a-Si & CdTe	To assess the energy performance of a ventilated PV double-skin façade (PV-DSF)	EnergyPlus simulation	Berkeley (USA)	65 kWh/m ² power output yearly from the a-Si based PV-DSF and doubled power output if using the CdTe based PV-DSF
Sun et al. (2018)	CdTe	To evaluate the energy and daylight performance	EnergyPlus & RADIANCE	Five cities in China	Up to 73% energy saving and lower possibility of glare compared to a conventional double glazing
Lee and Yoon (2018)	DSSC	To investigate the electrical characteristics under varying sky conditions	Outdoor experiment	Daejeon (South Korea)	Enhanced power conversion efficiency at a lower solar intensity
Chung et al. (2020)	DSSC	To analyse the correlations between DSSC window's characteristics and building energy performance.	DesignBuilder simulation	Seoul (South Korea)	Higher energy saving potential with enhanced PCE or visible light transmittance.
Cannavale, Ierardi, et al. (2017)	PSC	To examine the potential benefits of using PSC windows based on a real office building	DesignBuilder simulation	Bari (Italy)	18% reduction in overall electricity demand if replacing clear-glass windows with PSC windows
Bhandari et al. (2022)	PSC	To investigate the electrical, optical and visual performance of PSCs	Indoor experiment & calculation	Various climatic regions	Obvious changes in transparency, CCT and CRI when the cell temperature is greater than 55 °C

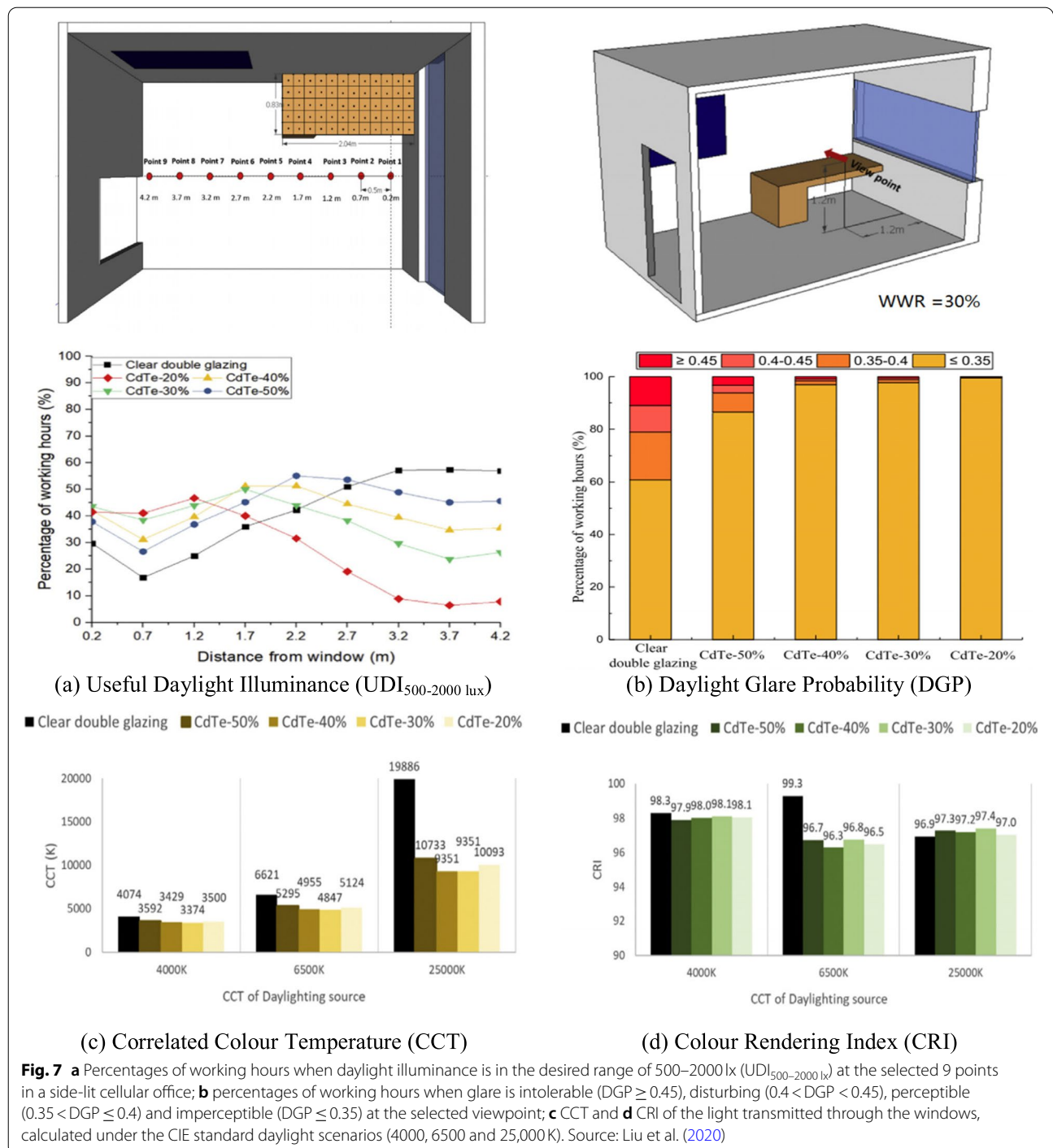


office (WWR=30%) under the climatic conditions of Birmingham (UK). If the task area is located close to the window, it is suggested to use a less transparent CdTe window in order to achieve higher percentages of annual working hours when the indoor illuminance level falls within the comfortable range 500–2000 lx (UDI_{500–2000 lx}) (see Fig. 7 (a)) and when glare is imperceptible (DGP ≤ 0.35) (see Fig. 7 (b)). For all the tested CdTe windows, the CCT values of transmitted daylight are within the recommended range (i.e., 3000–7500 K) under the daylight scenarios of 4000 K and 6500 K (see Fig. 7 (c)). Moreover, the CdTe windows can accurately display colours as their CRI values are above 95 (see Fig. 7 (d)). The above results indicate good potentials of CdTe glazing in reducing energy usage while maintaining visual quality in buildings.

Dye-sensitised Solar Cells (DSSCs) have gained widespread attention for their unique properties: inherent semitransparency, colour tunability (depending on the dye used), substrate flexibility, ability to operate in variable lighting conditions, and short payback periods (2–3 years), which make them a promising candidate for BIPV glazing applications (Cannavale, Ierardi, et al., 2017; Ghosh, 2020; Skandalos & Karamanis, 2015). However, their commercial uptake is still hindered by a few problems such as low PCE (up to 12%), chemical degradation and electrolyte leakage (Cannavale, Hörantner, et al., 2017; Sharma et al., 2018). To address challenges associated with low PCE, a variety of methods have been proposed, for example, co-sensitization for broadening the spectral response range (i.e., mixing two or more sensitising dyes with different absorption bands) (Rho et al., 2015; Sharma et al., 2018), and use of photoelectrodes constructed with nanostructures

(e.g., nanotubes and nanowires) to attain more effective charge transport/collection and reduce recombination losses (Sharma et al., 2018; Zhang & Cao, 2011). To overcome the volatilization and leakage problems of liquid electrolyte, DSSCs made of quasi-solid-state electrolytes and gel electrolytes have been developed (Sharma et al., 2018). Recent studies have reported the characteristics and efficacy of DSSC windows in terms of colour quality (Ghosh et al., 2018; Roy et al., 2019), glare protection (Selvaraj et al., 2019), long-term outdoor performance (Lee & Yoon, 2018) and building energy saving (Chung et al., 2020).

Perovskite solar cells (PSCs) have become a hot topic in recent years and shown remarkable progress with rapid improvements in PCE, from 3.8% in 2009 to above 25% in 2021 (Faheem et al., 2022; Kim & Kim, 2021). Perovskites are promising photoactive materials with unique features such as facile bandgap tunability via adjusting their compositions, high absorption coefficient, high charge carrier mobility, and low-cost material processibility (Faheem et al., 2022; Liu et al., 2018; Xue et al., 2018). The bandgap tuning enables the development of multi-junction (tandem) solar cell devices comprising two or more perovskites with different bandgap energies (i.e., all-perovskite tandem solar cells), or perovskites with established absorber materials (e.g., perovskite-silicon tandem solar cells), which can potentially harvest a broader range of incident photons from the solar spectrum and thus achieve higher PCEs than single-junction solar cells (Aydin et al., 2020; Li & Zhang, 2020; Unger et al., 2017). For example, the certified PCE of perovskite-silicon solar cells has reached 29.8% to date (National Renewable Energy Laboratory, 2022). Besides, the bandgap tuning of perovskites offers an effective approach to selectively



harvest the invisible parts of the solar spectrum including ultraviolet (UV) and near-infrared (NIR) radiation for power generation (Liu et al., 2018). This presents an enormous opportunity to realise high transparency in the visible region along with high PCE for semi-transparent PV

applications (Bhandari et al., 2022; Liu et al., 2018). The commercialisation potential of perovskite solar cells can be further enhanced once the concerns of their operational stability, scalable fabrication and toxicity are solved (Faheem et al., 2022, Xue et al., 2018).

3.2 Building integrated concentrating photovoltaic glazing

Low electric power output per unit solar cell area is one of the major barriers to the widespread adoption of BIPV systems. A viable solution to improve the rate of power generation is to incorporate a solar concentrator in BIPV design (Chemisana, 2011). The idea behind solar concentrators is to concentrate sunlight onto PV cell areas by using low-cost optical devices made of materials such as plastic, glass and mirror (Abu-Bakar et al., 2015; Shanks et al., 2016). For building integration, the majority of Concentrating Photovoltaics (CPV) systems are designed to be stationary with low concentration ratios (<10 suns) (Chemisana et al., 2016). Although CPVs with medium concentration ratios (10–100 suns) or high-concentration ratios (>100 suns) could potentially offer higher electric power output per unit solar cell area, they require one or two-axis tracking systems to cater for the sun movement and maximise the solar radiation collection through a day, which prevents them from architectural integration. A review on the suitability of CPVs for building integration was presented by Chemisana (2011).

A variety of concentrating optics have been proposed for BICPV applications, classified by geometric shape, including planar (or flat plate) and non-planar optical elements. Planar optical elements include diffused reflector (Kim & Dutta, 2012), holographic film (Kasezawa et al., 2016) and Luminescent Solar Concentrator (LSC) (Kerrouche et al., 2014a; Wiegman & Van Der Kolk, 2012). Non-planar optical elements include Fresnel lens (Zhu et al., 2018), wedge prism (Sabry, 2016; Yamada et al., 2011) and Compound Parabolic

Concentrator (CPC) (Sellami & Mallick, 2013). CPV systems based on such optical elements are generally designed and optimised using ray-tracing techniques (Baig et al., 2013). The following sub-sections describe the two categories of BICPV systems in detail in terms of their features and research findings.

3.2.1 Flat-plate static solar concentrators

Flat Plate Static Concentrators (FPSCs) usually feature a transparent planar waveguide with reflectors placed in between adjacent solar cells at the waveguide's backside, as illustrated in Fig. 8. The reflector can be in the form of a metal-coated v-grooved sheet (Uematsu, Yazawa, Tsutsui, et al., 2001; Yoshioka et al., 2003), a Lambertian diffused sheet (Morimoto & Maruyama, 2005; Smestad & Hamill, 1984; Weber et al., 2004) or a plate doped with luminescent species (Corrado et al., 2013; Leow, Corrado, Osborn, & Carter, 2013; Leow, Corrado, Osborn, Isaacson, et al., 2013). When light rays enter an FPSC, some rays are specularly reflected or scattered from the reflectors. A fraction of the reflected rays are trapped within the waveguide through Total Internal Reflection (TIR) and subsequently redirected to the solar cells for power generation. The light-trapping ability is determined by the critical angle of the waveguide (e.g., 42° for glass cover with a refractive index of 1.5 (Kim et al., 2016)) and also affected by the usage of secondary optical elements (e.g., mirrors and lenses at the waveguide's edges (Kim & Dutta, 2012)).

Uematsu, Yazawa, Joge, & Kokunai (2001), Uematsu, Yazawa, Tsutsui, et al. (2001) and Uematsu et al. (2003) proposed two FPSC modules consisting of v-grooved reflectors with monofacial solar cells (Fig. 8 (a)) and bifacial solar cells (Fig. 8 (b)), respectively. The short-circuit

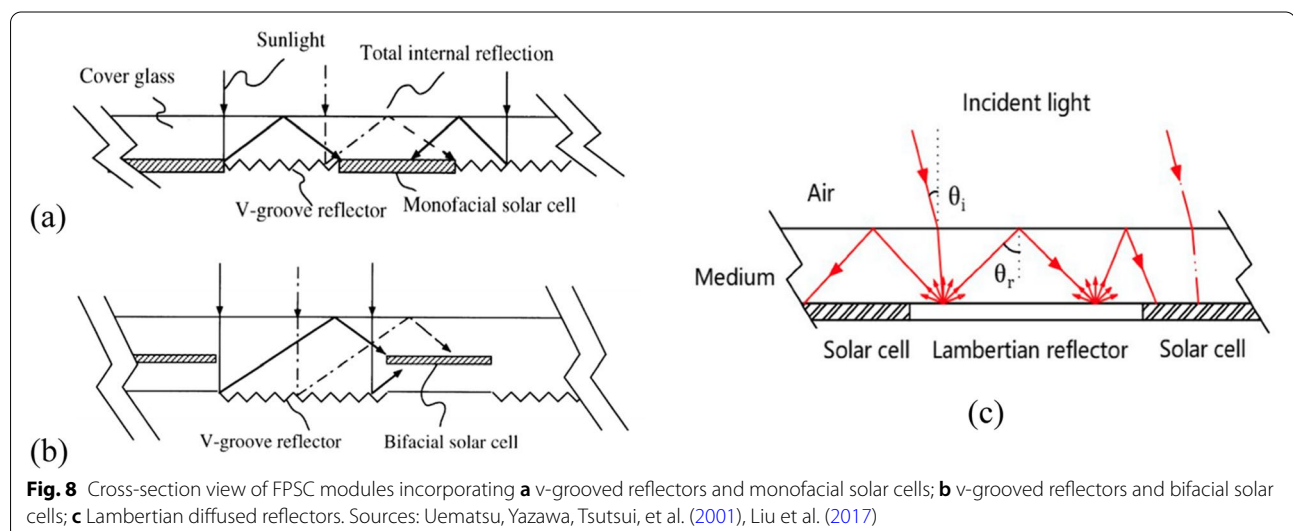


Fig. 8 Cross-section view of FPSC modules incorporating **a** v-grooved reflectors and monofacial solar cells; **b** v-grooved reflectors and bifacial solar cells; **c** Lambertian diffused reflectors. Sources: Uematsu, Yazawa, Tsutsui, et al. (2001), Liu et al. (2017)

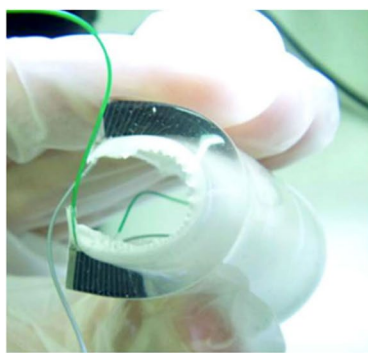
current densities of the monofacial-cell-type and bifacial-cell-type FPSC modules are respectively 1.31 and 1.71 times higher as compared to their counterparts without v-grooved reflectors. A further optimisation study of the monofacial-cell-type FPSC module was carried out by Yoshioka et al. (2003). The simulation result shows that the FPSC module with the optimised parameters, including a v-groove slope angle of 30°, a reflector width of 8 mm and a cell width of 14.5 mm, can reduce the coverage area of solar cells to 75% of a conventional PV module while achieving a similar power output. The findings of a ray-tracing study by Weber et al. (2006) reveal that the optical performance of FPSC modules based on v-grooved reflectors depends on the modules' elevation angle and orientation.

In contrast to v-grooved reflectors, Lambertian type diffused reflectors scatter light uniformly regardless of the angle of light incidence. Hence, a Lambertian-reflector based solar concentrator can provide similar optical concentration effects over a wide range of incidence angles (Liu et al., 2017; Weber et al., 2006). Chou et al. (2013) developed a flexible FPSC module consisting of a polydimethylsiloxane (PDMS) plate with edge-adhered poly-Si solar cells and a white-diffuse rear reflector, as shown in Fig. 9 (a). The white-diffuse rear reflector, which was made from another PDMS layer doped with TiO₂ nanoparticles, behaved as a near-Lambertian reflector. By ray-tracing simulation, it was found that the FPSC module has nearly constant optical concentration ratios (C_e) for incidence angles up to 50°, as shown in Fig. 9 (b). Moreover, the FPSC module with four poly-Si cells has an optical efficiency (η_o) of 35.07% and a PCE of 4.63%. Here, C_e is defined as the ratio of the irradiance (unit: W/m²) on the PV cell surface to that on the module aperture; η_o is defined as the ratio of the radiant energy flux (unit: W)

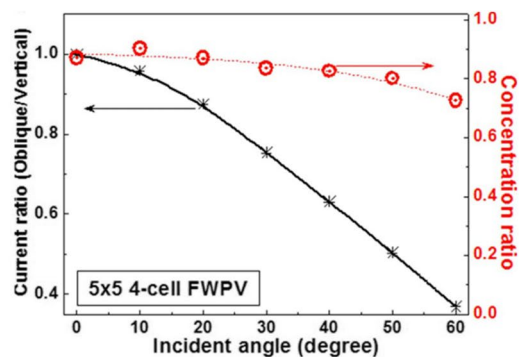
received by the solar cells to the flux incident on the module aperture.

Hezel (2003) proposed a new design of solar shading device based on bifacial solar cells in combination with a white semi-transparent rear reflector, as illustrated in Fig. 10 (a). The solar shading devices were installed with a tilt angle of 45° at the top of the south-oriented windows, to allow glare-free diffuse light to enter the office room, as shown in Fig. 10 (b). This design enables the collection of the solar radiation falling on the front sides of the bifacial cells as well as the light backscattered to the rear sides, which achieves up to 58% enhancement in power output compared to the monofacial-cell-type counterpart.

An FPSC module utilising Luminescent Solar Concentrator (LSC) panels as rear reflectors was introduced by Leow, Corrado, Osborn, & Carter (2013), Leow, Corrado, Osborn, Isaacson, et al. (2013) and Corrado et al. (2013). In contrast to the traditional LSC windows in which solar cells are attached along the perimeter of an LSC layer (Bergren et al., 2018; Kerrouche et al., 2014b; Zhang et al., 2015), the proposed system is constituted of a transparent acrylic waveguide with solar cells mounted front-facing and interspaced with LSC panels. As can be seen from Fig. 11 (a), the incident light is absorbed by the organic dyes (LR305) dispersed in the LSC panels and re-emitted isotropically, with a fraction redirected towards the solar cells through total internal reflection. The result of ray-tracing simulation in Fig. 11 (b) shows that the system yields a power gain of about 1.6 (i.e., about 60% increment in power output relative to the counterpart with no LSC panel) when the LSC distance between adjacent cells is increased to 10 cm. A further increase in LSC distance sees minor power gain improvement because of exacerbated optical losses by photon re-absorption and escaping (Leow, Corrado, Osborn, & Carter, 2013).

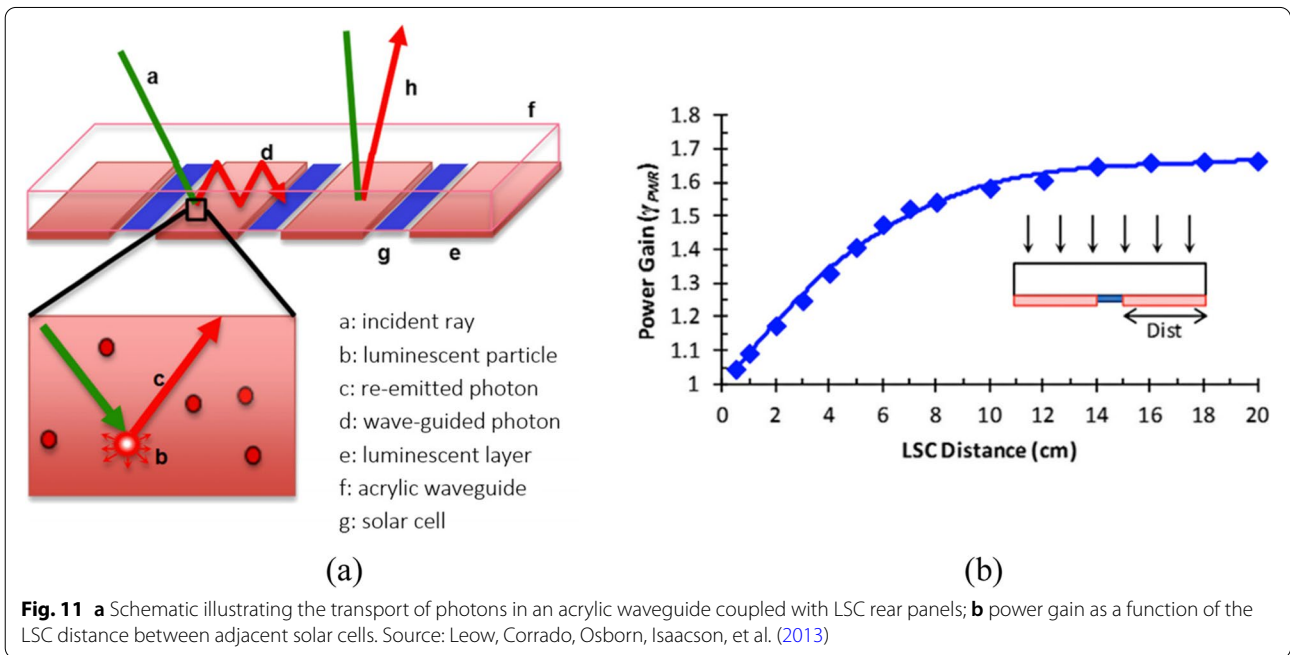
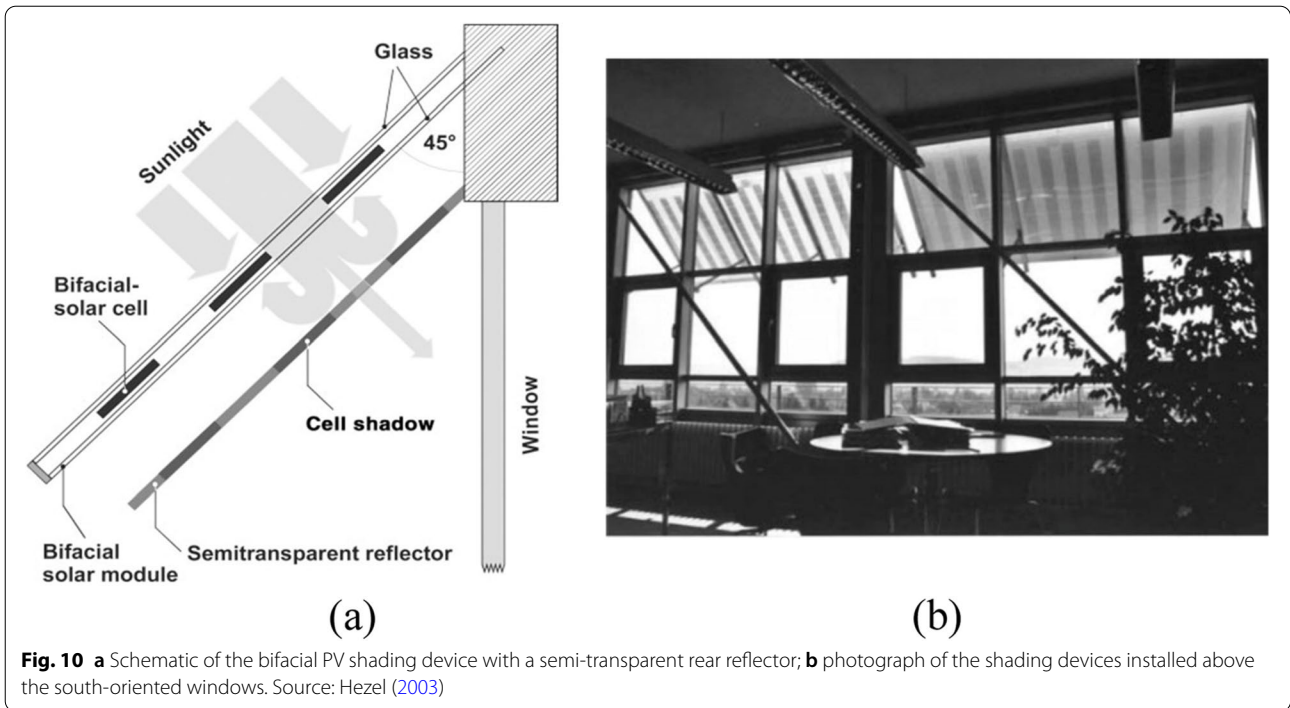


(a)



(b)

Fig. 9 **a** Photograph of a bendable FPSC module with a PDMS/TiO₂ composite bottom layer; **b** optical concentration ratio (red curve) of a 5 cm × 5 cm FPSC module with four poly-Si cells as a function of incidence angle. The optical concentration ratios are less than 1, because the solar cells were mounted at the module's edges where receive the light scattered from the white-diffuse rear reflector and have lower irradiances compared with the direct normal irradiance on the module's front aperture. Source: Chou et al. (2013)



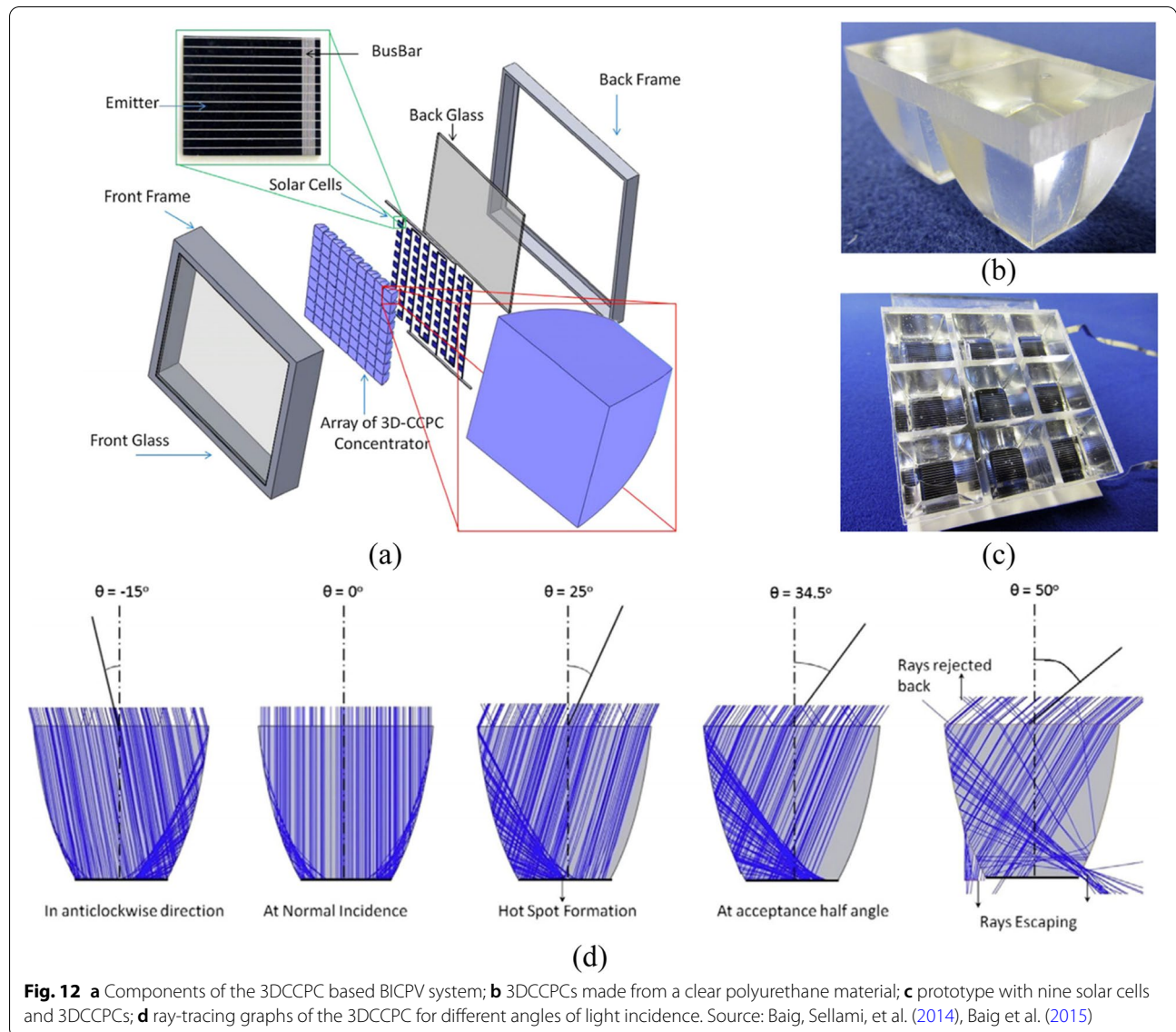
3.2.2 Dielectric based compound parabolic concentrator

A significant problem associated with FPSCs for window integration is their low transparencies caused by the use of highly reflective/scattering materials for the sake of attaining high optical concentration ratios. Transparent dielectric material based solar concentrators provide a

practical approach to improve PV power generation and allow the access of daylight. Dielectric based Compound Parabolic Concentrators (DiCPCs) forms a category of static solar concentrators widely studied, especially for building integration (Baig, Sarmah, et al., 2014; Yu et al., 2014). The reported dielectric materials for DiCPCs

include polycarbonate (Shanks et al., 2019), polyurethane (Baig, Sellami, et al., 2014), polymethyl-methacrylate (PMMA) (Baig et al., 2015) and Topas® (cyclic olefin copolymer) (Shanks et al., 2019), with high visible light transmittance (i.e., in the range of 70% to 90%) (Paul, 2011; Shanks et al., 2019). Different geometrical profiles of DiCPCs such as three-dimensional crossed CPC (Baig et al., 2015; Baig, Sellami, et al., 2014), rotational asymmetric CPC (Ramirez-Iniguez et al., 2017), linear asymmetric CPC (Mallick & Eames, 2007; Zacharopoulos et al., 2000) and lens-walled CPC (Su et al., 2012) have been introduced, and the DiCPCs' performance in terms of optical efficiency, I-V characteristics and temperature distribution have been investigated by numerical simulations and experiments.

Baig, Sellami, et al. (2014) and Baig et al. (2015) brought forward a CPV system based on 3D Crossed Compound Parabolic Concentrators (3DCCPCs), as shown in Fig. 12. An array of 3DCCPCs made from a clear polyurethane material (Crystal-clear 200®) were optically bonded to solar cells using an encapsulation material (Sylguard-184), and the bonded units were placed between two glass panes. Figure 12 (d) illustrates the trajectories of light rays entering a 3DCCPC at different incidence angles. The ray-tracing simulation results show that the 3DCCPC has a 34.5° acceptance half-angle (i.e., the incident angle at which the optical flux reaching the exit aperture falls to 90% of its maximum (Baig, Sellami, et al., 2014, Sharaf & Orhan, 2015)), combined with a maximum optical efficiency of 73.4%.



The maximum power output of the CPV system was found to be 2.65 times higher than that of its counterpart without 3DCCPCs at normal light incidence.

The research team at the University of Exeter (Baig et al., 2013; Baig, Sarmah, et al., 2014; Sarmah et al., 2014; Sarmah & Mallick, 2015) developed a CPV system consisting of linear Asymmetric Compound Parabolic Concentrators (ACPCs), as shown in Fig. 13. The designed ACPCs allows the incident light within the range of acceptance angles (0° - 55°) to be efficiently collected for power generation, and in the meantime, allowing some light to escape at the air-dielectric interfaces and transmit through the system for daylighting purposes. The outcome from an indoor experiment shows that the CPV system has a maximum optical efficiency of 80.5% and

a maximum power ratio of 2.27 (i.e., the ratio of power output relative to a non-concentrating counterpart) at the incidence angle of 20° (Sarmah et al., 2014). The CPV system was further characterised by an outdoor experiment in Edinburgh under different weather conditions (sunny, cloudy and rainy). An average power ratio of 2.19 was reported for the CPV system tested on a sunny interval day in October.

Despite the significant increment in power output, the use of dielectric CPCs usually leads to high solar cell temperature and non-uniform illumination on the solar cell surface (Baig et al., 2013; Baig, Sellami, et al., 2014). Baig et al. (2013) simulated the thermal and electrical performance of the linear ACPC system (Fig. 13) under the standard solar irradiation (AM1.5, 1000 W/

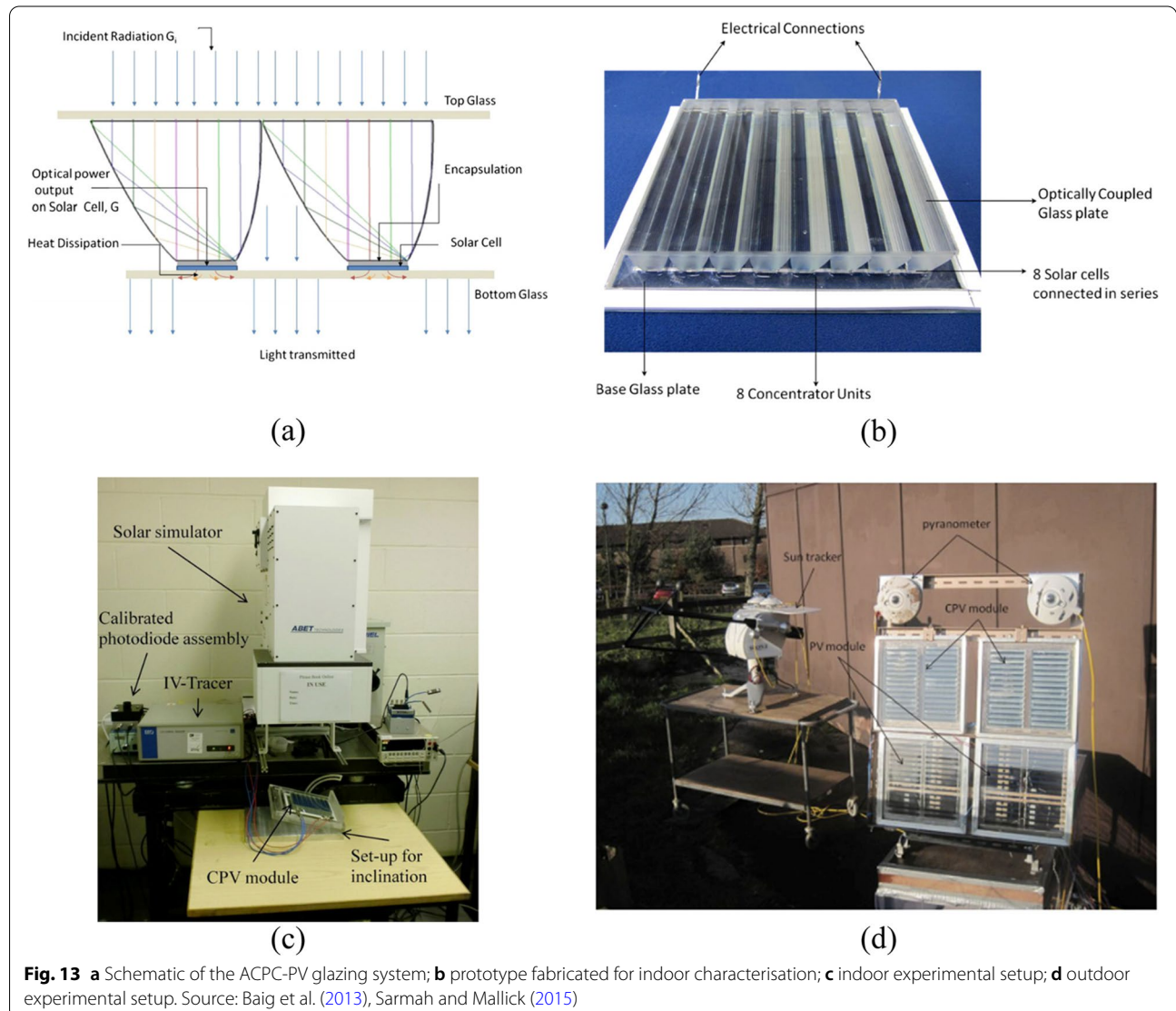


Fig. 13 a Schematic of the ACPC-PV glazing system; b prototype fabricated for indoor characterisation; c indoor experimental setup; d outdoor experimental setup. Source: Baig et al. (2013), Sarmah and Mallick (2015)

m²). A 51 °C maximum increase in solar cell temperature was observed, which brought down the power conversion efficiency from 18.5% (at 23 °C) to 15.6% (at 74 °C). The non-uniformity in flux distribution along the solar cell tends to cause detrimental hot spots, current mismatch and degradation in cell performance (Baig et al., 2013; Chemisana, 2011). The overheating problem can be relieved by combining the CPV systems with passive cooling mechanisms such as natural ventilation and Phase Change Material (PCM) (Sharma et al., 2016). However, these would increase cost and complexity with regards to architectural integration.

4 Thermotropic smart glazing technologies

Smart windows can change their optical properties reversibly to adapt to time-varying weather conditions or user requirements, hence offering selective and dynamic modulation of incoming solar radiation (Casini, 2018; Piccolo & Simone, 2015). Such functionality has become possible by integrating windows with chromogenic materials (e.g., thermochromic, photochromic, electrochromic and gasochromic), Suspended Particle Devices (SPD) and Polymer Dispersed Liquid Crystals (PDLC) (Baetens et al., 2010; Casini, 2018). There have been a number of review articles published on the topics of electricity-triggered smart windows (i.e., EC, SPD and PDLC smart windows) (Baetens et al., 2010; Casini, 2018; Granqvist, 2007) and thermochromic windows (Aburas et al., 2019; Cui et al., 2018; Kamalisarvestani et al., 2013).

Thermo-responsive materials which modulate optical transmittance via a tuneable light-scattering behaviour are usually denoted as ‘thermotropic materials’, in distinction to ‘thermochromic materials’ which are characterised by a change in colour between bleached (light) and tinted (dark). When used in windows, thermotropic materials offer an interesting possibility for the adaptive control of solar heat and visible light into buildings. In other words, the visible light transmittance and solar transmittance of thermotropic windows change with the diurnal and seasonal variations of weather conditions such as ambient air temperature and solar irradiation level. This feature can help in reducing the energy consumption for space cooling in summer without compromising much of the solar radiation for space heating and daylighting in winter. In addition, because thermotropic windows act on the basis of reflective and scattering effects, they can more effectively reduce the risks of direct-light glare and overheating than chromogenic smart windows (Seeboth et al., 2010). On the other hand, the tuneable scattering behaviour of thermotropic windows depends on the surrounding environmental conditions and cannot be actively controlled,

therefore they are not suitable for building areas where permanent viewing from the inside out is required (Allen et al., 2017).

In the following sub-sections, smart windows based on thermotropic hydrogel materials are described in more detail with regard to working mechanism (Section 4.1), dynamic optical characteristics (Section 4.2) and window performance in buildings (Section 4.3).

4.1 Working mechanism of thermotropic hydrogels

Thermotropic hydrogels are water (or solvent) poured cross-linked polymer networks with both hydrophilic and hydrophobic groups within their structures (Allen et al., 2017; Resch & Wallner, 2009). Figure 14 illustrates the reversible transition of a poly(N-isopropylacrylamide) (PNIPAm) based hydrogel between a transparent state and a translucent state during heating and cooling. Below the transition temperature (approximately 32 °C), also referred to as Lower Critical Saturation Temperature (LCST), the PNIPAm polymer is hydrophilic with hydrogen bonds prevailing between the polymer chains and water molecules. The polymer and water are mixed homogeneously at a molecular level; therefore, the hydrogel has a median refractive index and is highly transparent (Muehling et al., 2009; Resch & Wallner, 2009). Once the hydrogel temperature goes above the LCST, the polymer-water hydrogen bonds break, and the hydrophobic polymer-polymer interactions become dominant (Allen et al., 2017). Subsequently, phase separation occurs with the polymer chains aggregating and free water quenched out from the polymer network. Therefore, light scattering takes place at the interfaces between the aggregated polymer particles (scattering domain) and the free water (matrix) which have different refractive indices (Muehling et al., 2009; Seeboth et al., 2010) (see Fig. 15), resulting in a translucent appearance of the hydrogel.

In practical terms, the thermotropic hydrogel used in a smart window needs to fulfil several requirements (Seeboth et al., 2000, Schneider & Seeboth, 2001, Resch & Wallner, 2009, Zhou et al., 2014, Allen et al., 2017):

- High visible light transmittance (380–780 nm) (> 70%);
- Near-room-temperature transition (between 25 and 35 °C);
- Steep switching gradient (< 10 °C);
- High reversibility and low hysteresis in the heating-cooling process;
- High viscosity to distribute the internal hydrostatic pressure evenly in the interspace of a glazing unit and not to run out;
- Non-toxic, non-freezing, stable against UV radiation;
- Low cost and good scalability.

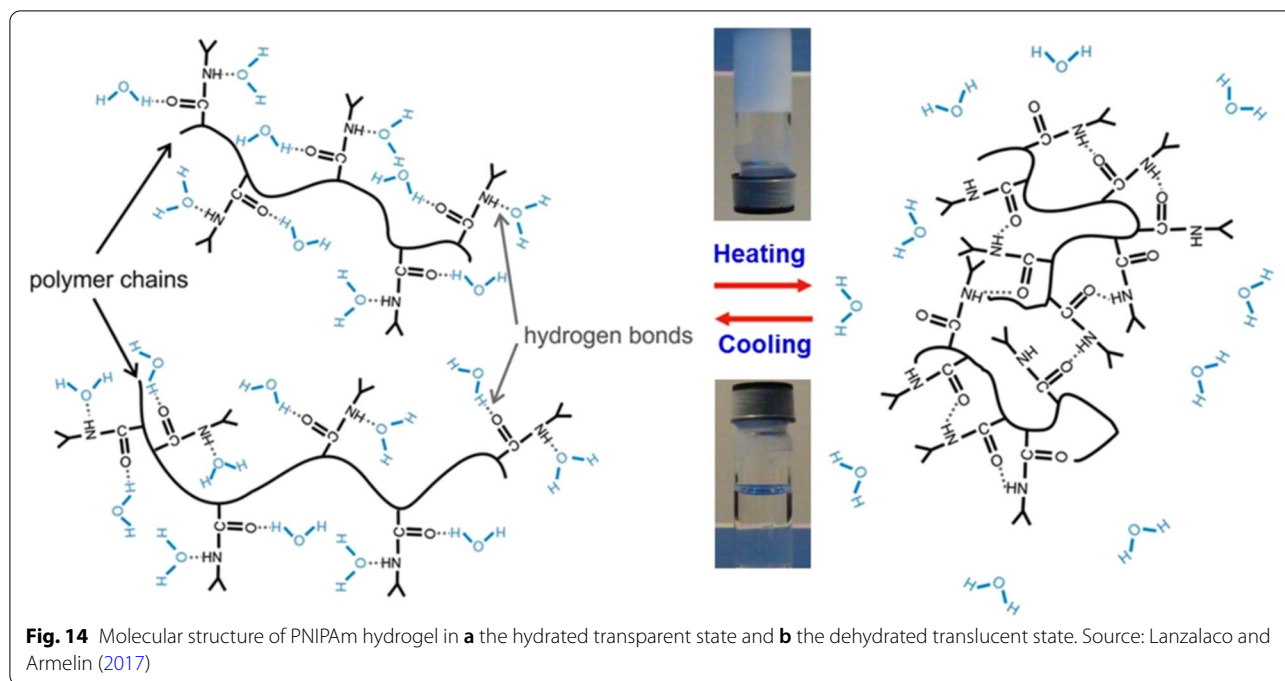


Fig. 14 Molecular structure of PNIPAm hydrogel in **a** the hydrated transparent state and **b** the dehydrated translucent state. Source: Lanzalaco and Armelin (2017)

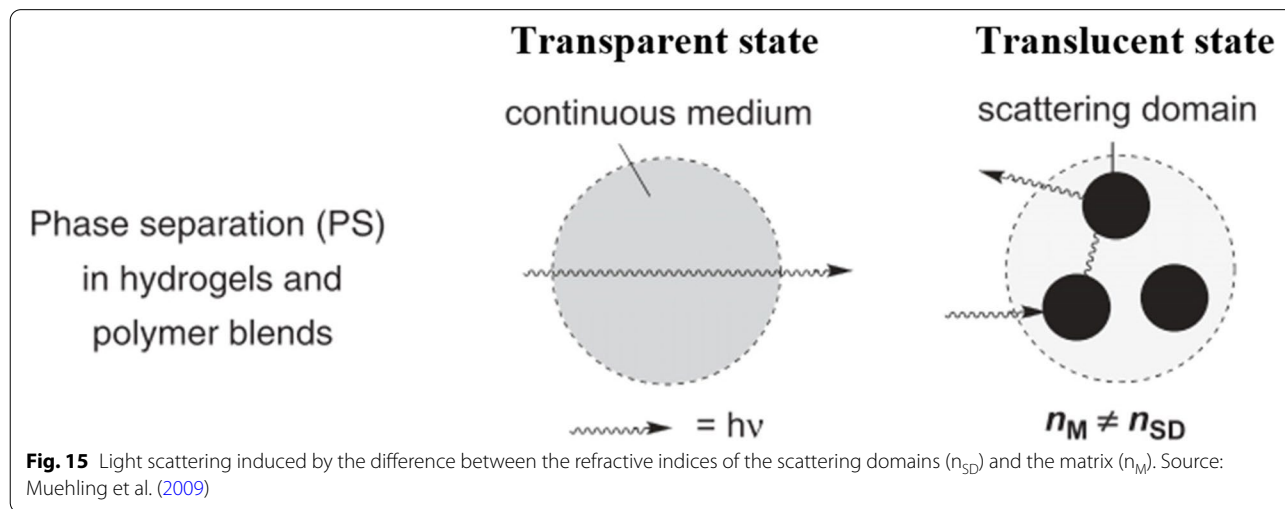


Fig. 15 Light scattering induced by the difference between the refractive indices of the scattering domains (n_{SD}) and the matrix (n_M). Source: Muehling et al. (2009)

4.2 Dynamic optical characteristics of thermotropic hydrogels

Thermotropic hydrogels are commonly produced from synthetic polymers or biopolymers (Resch & Wallner, 2009). As a typical member of synthetic polymers, poly(N-isopropylacrylamide) (PNIPAm) has been extensively investigated due to its unique features, such as reversible abrupt transparent-opaque transition, good resistance to UV radiation and simplicity of synthesis (Maiorov, 2020; Wang et al., 2014). Pure PNIPAm hydrogels have an LCST of approximately 32 °C

(Nun et al., 2017). The LCST of PNIPAm hydrogels is tuneable with the approaches including copolymerisation (Jin et al., 2013; Mizuntani et al., 2011), adding co-solvents (Wang et al., 2014) and adding salts (Du et al., 2010). Mizuntani et al. (2011) prepared PNIPAm hydrogels with LCST in the range of 25 °C and 40 °C by copolymerising with hydrophobic amide-monomer (to increase LCST) or hydrophilic ester-monomer (to decrease LCST). Wang et al. (2014) proposed PNIPAm microgel colloids based on a binary solvent of water and glycerol mixture. The LCST was found to

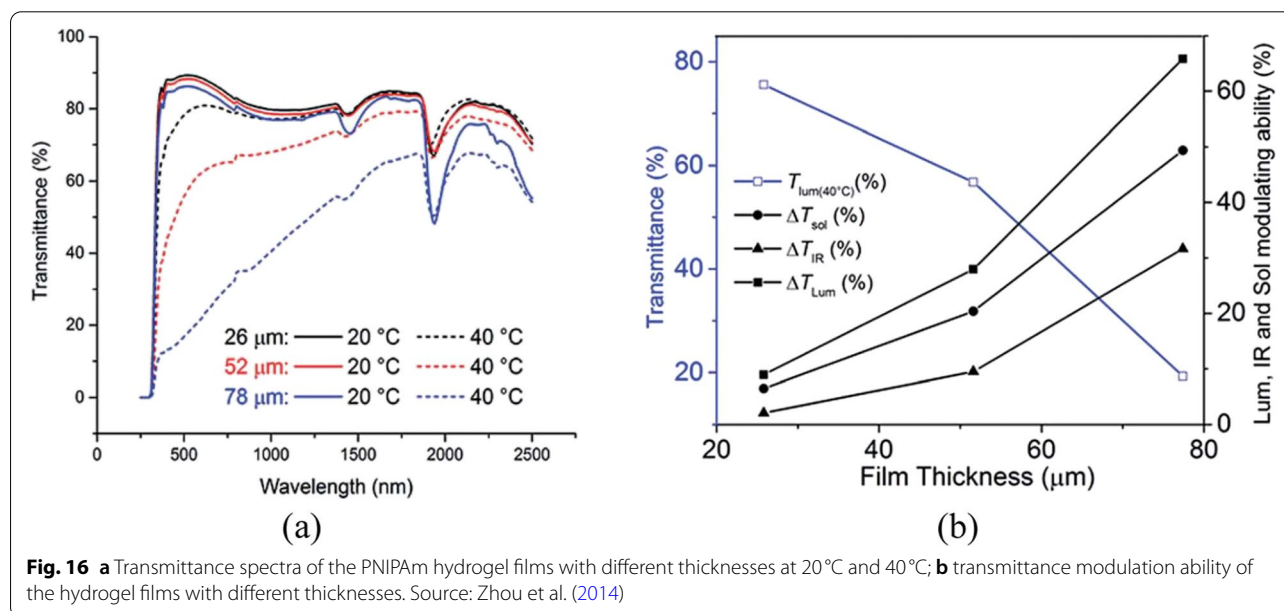
decrease from 32.2 °C to 20.4 °C by increasing the glycerol content from 0 wt% to 35 wt% (of total solvent). The researchers also found that adding glycerol co-solvent can enhance the freezing tolerance and reduce the water evaporation rate of PNIPAm hydrogels (Wang et al., 2014).

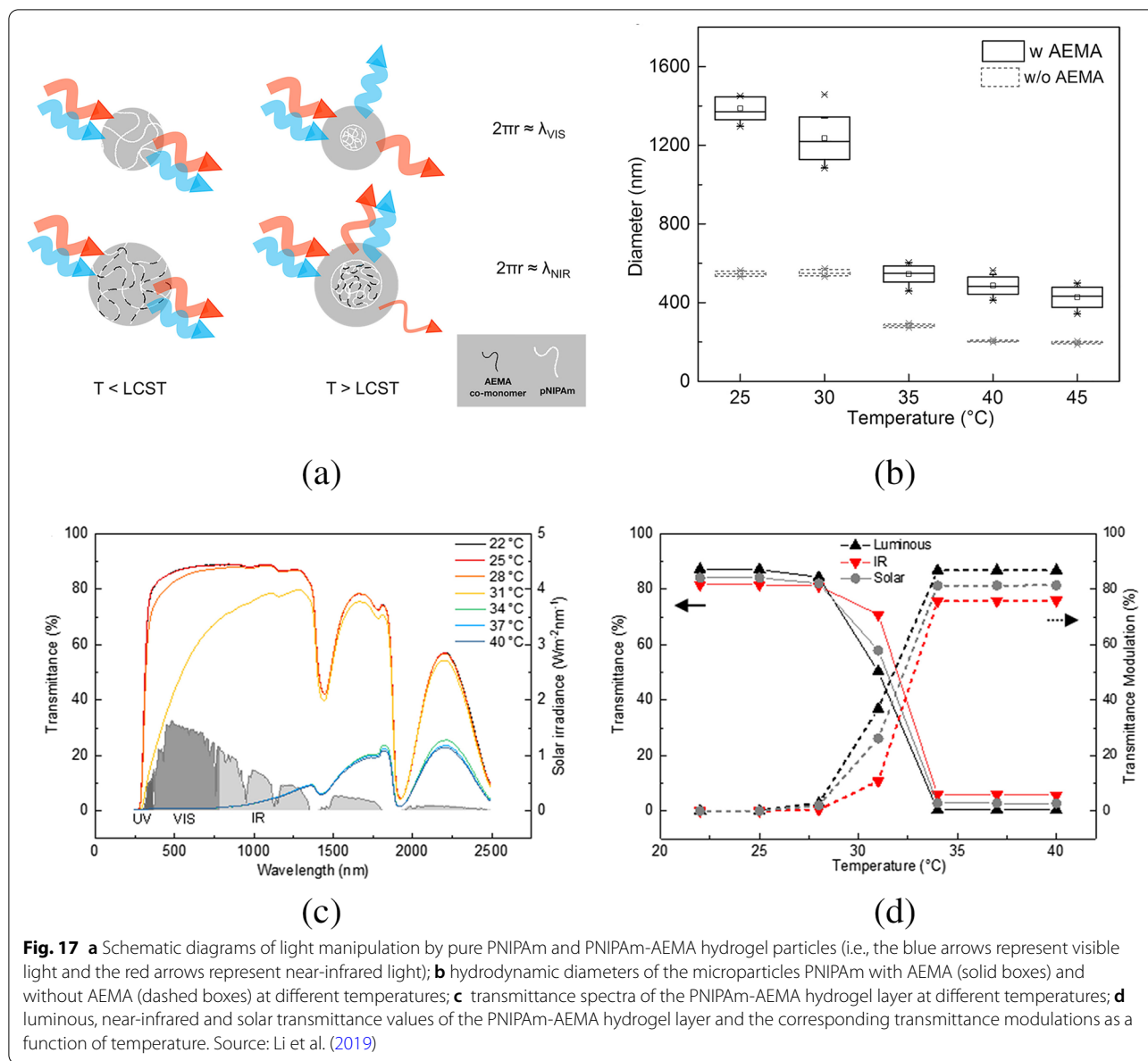
Zhou et al. (2014) fabricated a TT glazing unit consisting of a micrometre thick PNIPAm hydrogel film (LCST = 32 °C) laminated between two pieces of glass, and measured its optical performance with respect to different film thicknesses (26, 52 and 78 μm). As can be seen from Fig. 16, in the cold state (20 °C) all the three samples have similarly high transmittance values over the whole solar spectrum (250–2500 nm). In the hot state (40 °C) the samples with larger thicknesses exhibit lower spectral transmittance values together with stronger transmittance modulation ability (i.e., the optical transmittance difference between the cold and hot states). For the 78-μm-thick-hydrogel sample, the transmittance modulations in the luminous region (380–780 nm, ΔT_{lum}), the near-infrared region (780–2500 nm, ΔT_{IR}) and the solar spectrum (250–2500 nm, ΔT_{sol}) are 65.9%, 31.7% and 49.6%, respectively. The relatively ineffective light shielding in the NIR region may be attributed to the small PNIPAm particle sizes that are not comparable to the wavelengths of the NIR spectral range (Gladden et al., 2015; Li et al., 2019).

Li et al. (2019) demonstrated a smart window with an interlayer of poly(N-isopropylacrylamide)-2-aminoethylmethacrylate hydrochloride (PNIPAm-AEMA) hydrogel microparticles (LCST \approx 32 °C). The hydrogel microparticles were prepared by co-polymerizing

PNIPAm and AEMA via a continuous feeding solution-phase synthesis. The purpose of utilising AEMA as a co-monomer in the hydrogel synthesis is to increase the particle size so as to achieve a stronger IR transmittance modulation compared with pure PNIPAm hydrogel (Jiang et al., 2021; Li et al., 2019), as explained in Fig. 17 (a). For example, the hydrodynamic diameters of the PNIPAm hydrogels without and with AEMA at 35 °C are 282 nm and 546 nm respectively (see Fig. 17 (b)), the latter of which contributes to a particle size parameter ($2\pi r/\lambda$) comparable to 1 in the NIR region, indicating more effective NIR light scattering. The transmittance modulations of the 240-μm-thick PNIPAm-AEMA hydrogel layer were measured to be 87.2% in the visible region, 75.6% in the near-infrared region and 81.3% over the solar spectrum, as shown in Fig. 17 (c) and (d).

Recent attempts were considering natural hydrogels based on cellulose derivatives, such as Hydroxypropyl Cellulose (HPC) (Connelly et al., 2016; Connelly et al., 2017; Yang et al., 2016) and Hydroxypropyl Methyl Cellulose (HPMC) (Cao et al., 2018; Yao & Yan, 2010), for the development of thermotropic windows. HPC is a non-toxic, biodegradable, water-soluble solid polymer (Resch & Wallner, 2009; Yang et al., 2016). Its advantages over synthetic polymers regarding price and availability make it economically feasible for large scale applications (Resch & Wallner, 2009). Furthermore, the scattering domain sizes of HPC hydrogels could reach as high as 1–2 μm in diameter; therefore, radiation in both the visible and NIR regions can be effectively scattered (Maiorov, 2020; Yang et al., 2016). As illustrated in Fig. 18, the HPC aqueous solution turns cloudy and milky-white at temperatures

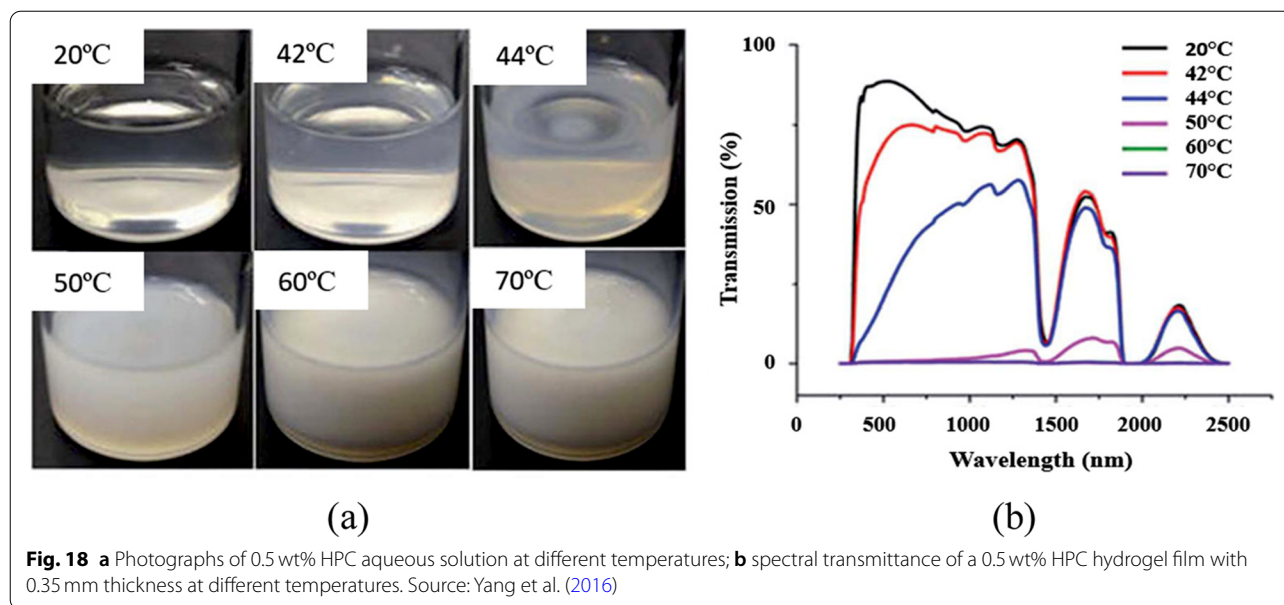




above 42 $^{\circ}C$. The HPC hydrogel layer at 70 $^{\circ}C$ becomes nearly opaque to light over a broad range of the solar spectrum.

Watanabe (1998, 2007) developed an Affinity Intelligent WindowTM with a glazing aperture area of 1 m². The thermotropic hydrogel laminated between two glass panes was synthesised of HPC, water, sodium chloride and an amphipathic compound, the last of which acts as a spacer to avoid the irreversible sedimentation of HPC aggregates during phase separation. Schneider and Seeboth (2001) suggested integrating HPC with Hydroxyethyl Cellulose (HEC) or gellan gum instead of an amphipathic substance to prevent ageing (Resch & Wallner, 2009).

Connelly et al. (2016) developed thermotropic hydrogels based on different concentrations of HPC polymer (2, 4 and 6 wt%) and gellan gum gelling agent (0.8, 1.2 and 1.5 wt%). As can be seen from Fig. 19, the spectral transmittance (at 600 nm) of the 6 wt% HPC and 1.5 wt% gellan gum hydrogel membrane reduces to ~20% and the spectral reflectance rises to ~50% with the membrane temperature increasing to 60 $^{\circ}C$. Using a lower HPC concentration of 4 wt% or 2 wt% results in higher transmittance and lower reflectance in the translucent states (i.e., at temperatures above the transition point ~42 $^{\circ}C$), indicating the effectiveness of HPC concentration in changing the hydrogel's light-scattering performance. On the



other hand, changing the HPC concentration has a minor effect on the hydrogel's transition temperature.

The isotropic-to-biphasic transition temperature or cloudy point of a salt-free aqueous solution of ≤ 40 wt% HPC is around 40°C , as shown in Fig. 20. Adding salt enables the cloudy point to shift down or up depending on the sorts of the associated anion and cation (Nishio et al., 2002) (see Fig. 20). For instance, the cloudy point of HPC aqueous solution can be decreased from 42°C to 20°C by increasing the content of sodium chloride (NaCl) salt from 0 to 1.4 mol/litre (Xia et al., 2003).

4.3 Design and numerical evaluation of thermotropic windows

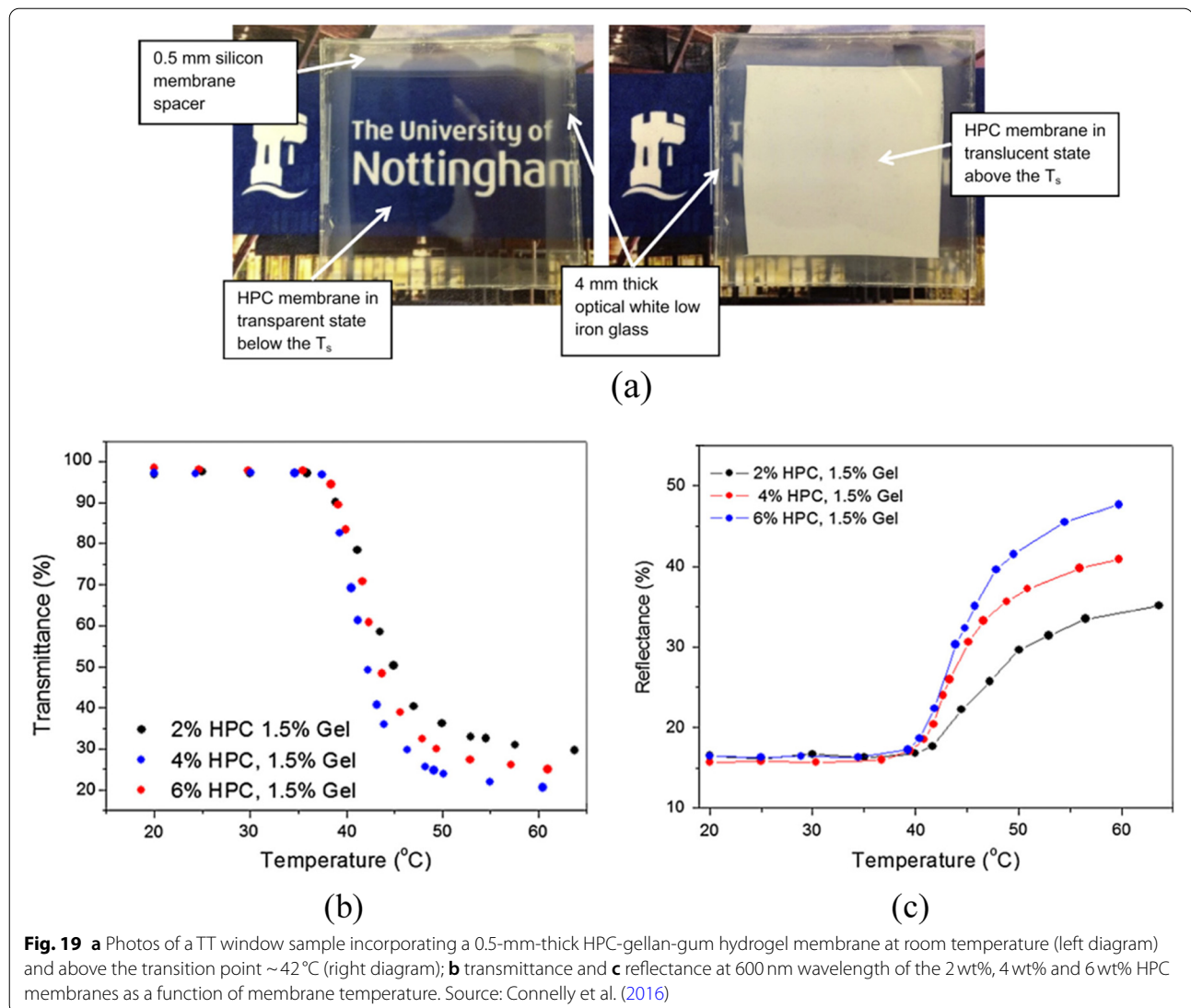
A thermotropic (TT) window can be simply manufactured by filling the intervening space between two glass panes with a thermotropic hydrogel material and then sealing around the edges. If the TT window is intended to be used in regions with cold winters, it is usually combined with one or more additional glass pane(s) with a low-emissivity (low-E) coating(s) for enhanced thermal insulation (Nitz & Hartwig, 2005) (see Fig. 21 (a)). To facilitate satisfactory views into and out of a building, a TT smart window/facade can be designed with switchable glazing mounted in the upper (or side) section and visually clear glazing mounted in the lower (or middle) section, such as the examples shown in Fig. 21 (b) and (c).

Yao and Zhu (2012) proposed a smart window comprising an HPMC-NaCl based hydrogel membrane ($\text{LCST} = 31^\circ\text{C}$) between two clear glass panes, and numerically analysed the window's effect on the energy consumption and thermal comfort inside a residential

building under the climatic conditions of Hangzhou (China). The results suggest that installing the smart windows on the west-facing façade ($\text{WWR} = 30\%$) can potentially reduce the risk of thermal discomfort due to space overheating by 70%, while cutting the annual cooling energy consumption by 19%, in comparison with the use of conventional double-glazed windows.

Allen et al. (2017) evaluated the effectiveness of HPC-based TT glazing units with different tilt angles and transition temperature ranges in reducing undesirable solar heat gain and energy consumption for buildings in the hot summer Mediterranean climate of Palermo (Italy). At the tilt angle of 0° (i.e., horizontal skylight), the TT glazing unit with a transition temperature range of $40\text{--}50^\circ\text{C}$ can reduce the annual total energy consumption by approximately 22%, compared to an ordinary double-glazing unit. No significant improvement in total energy saving was observed when reducing the transition temperature range, for example, to $35\text{--}45^\circ\text{C}$ or below. This can be attributed to the increasing energy consumption for space heating and artificial lighting, which compensates for the reduction in cooling load.

Zhou et al. (2020) demonstrated a $100\text{ cm} \times 100\text{ cm}$ smart window in a sandwich structure where the interspace between two clear glass panes was filled with a thermo-responsive PNIPAm liquid, as shown in Fig. 22 (a). Similar window samples at a smaller scale ($20\text{ cm} \times 20\text{ cm}$) with different PNIPAm liquid thicknesses (1 cm, 1 mm and 0.1 mm) were developed for optical characterisations. As can be seen from Fig. 22 (b) and (c), the transmittance modulation capability becomes stronger when a thicker PNIPAm liquid is used, for



example, the luminous transmittance modulation (ΔT_{lum}) and solar transmittance modulation (ΔT_{sol}) of the 1-mm-liquid sample are $\sim 15\%$ and $\sim 11\%$ respectively, while the ΔT_{lum} and ΔT_{sol} of the 1-cm-liquid sample are $\sim 90\%$ and $\sim 68\%$ respectively. By EnergyPlus simulation, it is revealed that the 1-cm-liquid smart window with the strongest solar modulation ability gives the lowest HVAC energy consumption, which is $\sim 45\%$ less than that for the normal double-glazed window in the climate of Singapore (see Fig. 22 (d)).

Sun, Liu, et al. (2021) and Sun, Wilson, et al. (2021) proposed a TT PS-TIM window system that coupled a thermotropic (TT) material and a Parallel Slat Transparent Insulation Material (PS-TIM) structure to deliver high thermal resistance as well as daylighting control in an automatic/semi-automatic manner. In principle, the

TT PS-TIM window system can control the admission of daylight into the building space through the temperature-dependent optical switching of the integrated TT slats as well as the manual/automatic adjustment of the slat tilt angle, as depicted in Fig. 23 (a) and (b). Moreover, the PS-TIM structure can suppress the convective heat transfer between the external and internal glass panes enabling better thermal insulation. The result of $\text{UDI}_{500-2000 \text{ lx}}$ prediction suggests that the visual comfort of occupants can be enhanced by applying the TT PS-TIM window system with an appropriate slat tilt angle, as shown in Fig. 23 (c). From Fig. 23 (d), it is found that the maximum energy saving provided by the TT PS-TIM window system is 21.5% over a conventional double glazing, when using a slat tilt angle of 0° (i.e., horizontal) and a transition temperature of 25°C .

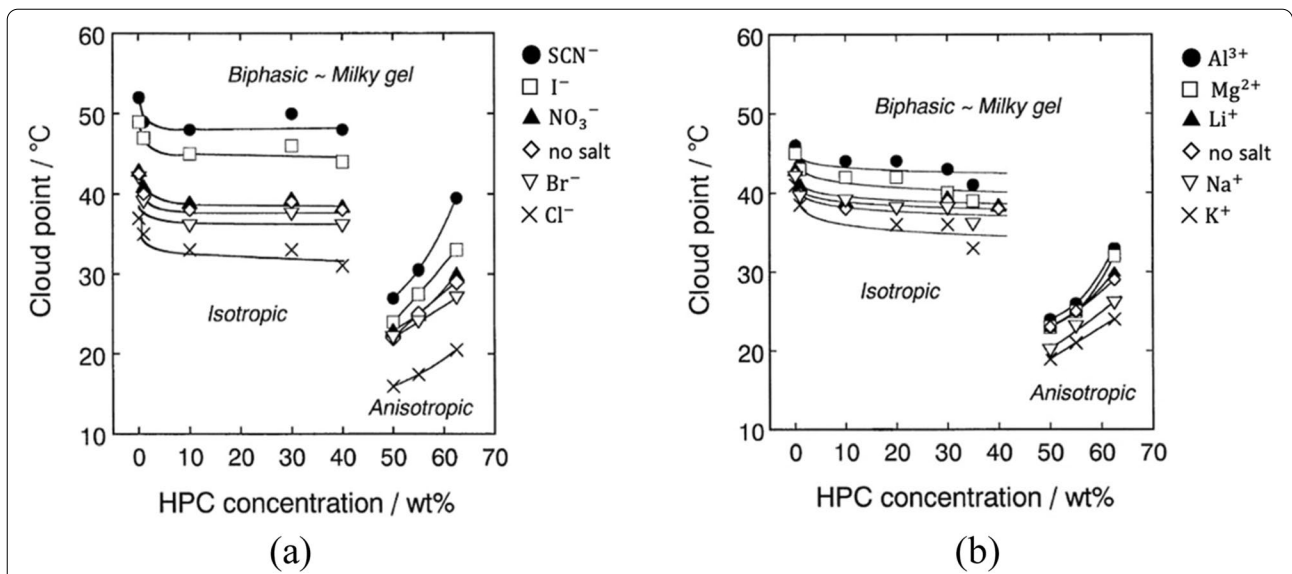


Fig. 20 Cloudy points of the HPC aqueous solutions added with **a** lithium salts with different anions and **b** metallic nitrates with different cations, at a salt concentration of 0.5 mol/litre. Source: Nishio et al. (2002)

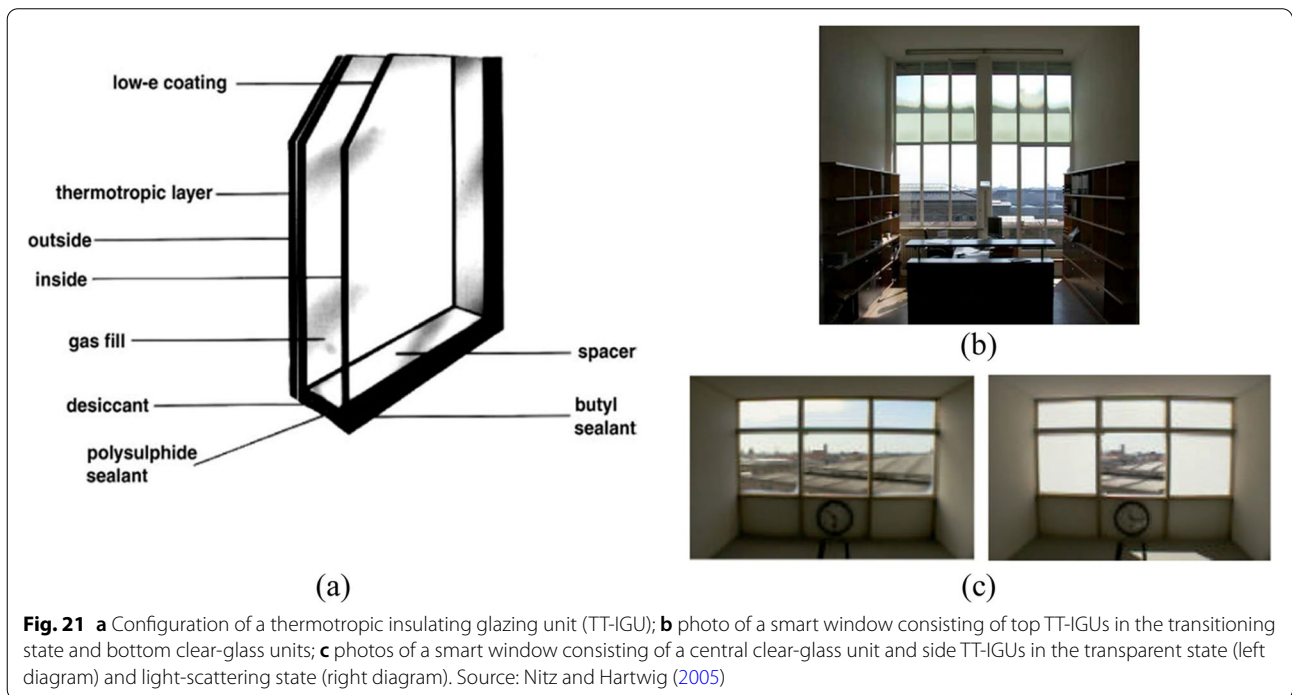


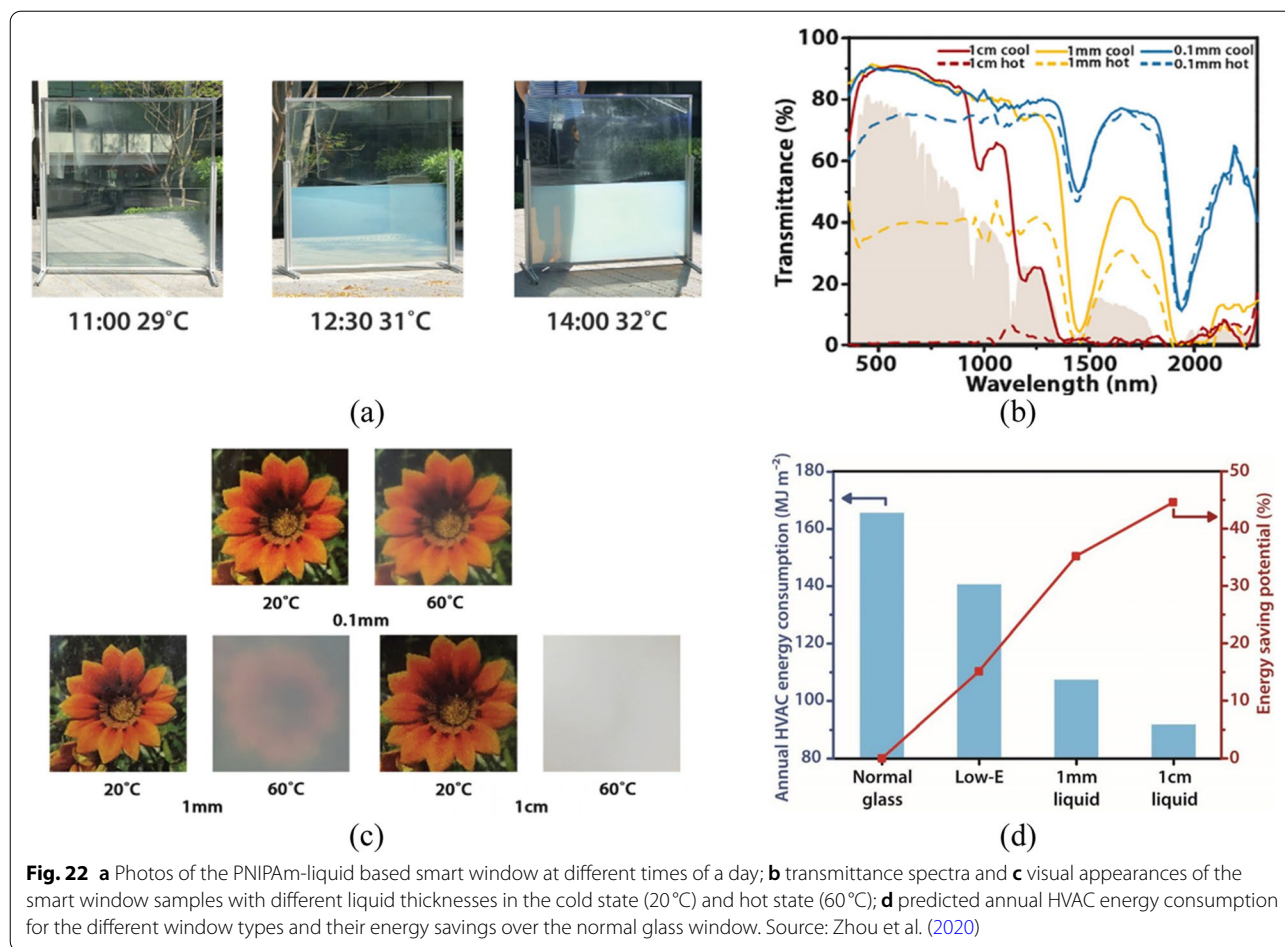
Fig. 21 **a** Configuration of a thermotropic insulating glazing unit (TT-IGU); **b** photo of a smart window consisting of top TT-IGUs in the transitioning state and bottom clear-glass units; **c** photos of a smart window consisting of a central clear-glass unit and side TT-IGUs in the transparent state (left diagram) and light-scattering state (right diagram). Source: Nitz and Hartwig (2005)

5 Dynamic glazing technologies for both electricity generation and daylighting control

The combination of BIPV window and smart window has given rise to a new discipline, termed BIPV smart window. Over the last decade, several innovative ideas have been put forward by combing semi-transparent PVs with

optically switchable materials, for example, PV-EC windows (Favoio et al., 2016; Ma & Chen, 2012), PV-LC windows (Ghosh et al., 2019; Kwon et al., 2015; Murray et al., 2016) and PV-TC windows (Guo et al., 2015; Lin et al., 2018).

Ma and Chen (2012) presented a self-powered smart window comprising a front c-Si PV panel and a back



electrochromic stack which consisted of four layers: indium tin oxide (ITO)-coated glass, tungsten oxide (WO_3), electrolyte and ITO-coated glass, as shown in Fig. 24 (a). The EC stack can be tuned between a fully darkened state and fully bleached state under the voltage (in the range of 0–3.5 V) supplied by the front PV panel via a voltage controller. Murray et al. (2016) developed a smart window based on a Polymer Dispersed Liquid Crystals (PDLC) device for daylighting control, which can be self-powered by an a-Si absorbing layer deposited on the glass coverslip, as shown in Fig. 24 (b). The PDLC device scatters incident light in the absence of an electric field (0 V, OFF state) and is transparent to visible light under applied voltage (150 V, ON state). The visible light transmittance values are 41% and 68% for the smart window in the OFF and ON states, respectively. However, concerning its limited transmission modulations over visible light and NIR radiation, the PV-PDLC smart window may not be fully competent to address glare and overheating problems. Moreover, most of commercially available PDLC films demand a comparatively high voltage in order to

maintain their transparent states, which could result in high electricity consumption and also a potential safety risk (Li et al., 2020).

Wheeler et al. (2017) demonstrated a photothermally modulated PV window with high visible light transmittance (up to 68%), high power conversion efficiency (up to 11.3%) and fast switching time (less than 3 min). The PV window has a switchable absorber layer made of methylammonium lead iodide-methylamine complex ($\text{CH}_3\text{NH}_3\text{PbI}_3 \cdot x\text{CH}_3\text{NH}_2$), the formation or dissociation of which changes the PV window to a bleached state (63% τ_{vis}) or a coloured state (3% τ_{vis}), respectively, as presented in Fig. 25 (a) and (b). The phase transition depends on the partial pressure of CH_3NH_2 gas (g) and the temperature of $\text{CH}_3\text{NH}_3\text{PbI}_3 \cdot x\text{CH}_3\text{NH}_2$ solid (s), described by the below equation. In the cold, bleached state, the PV window did not exhibit visible colour; when being exposed to solar illumination, the PV window was heated up and undergoing a colour change from yellow-orange to dark red (see Fig. 25 (d)), with an increase in short-circuit current density up to 21.2 mA/cm² under standard test conditions (1000 W/m², AM1.5) (see Fig. 25

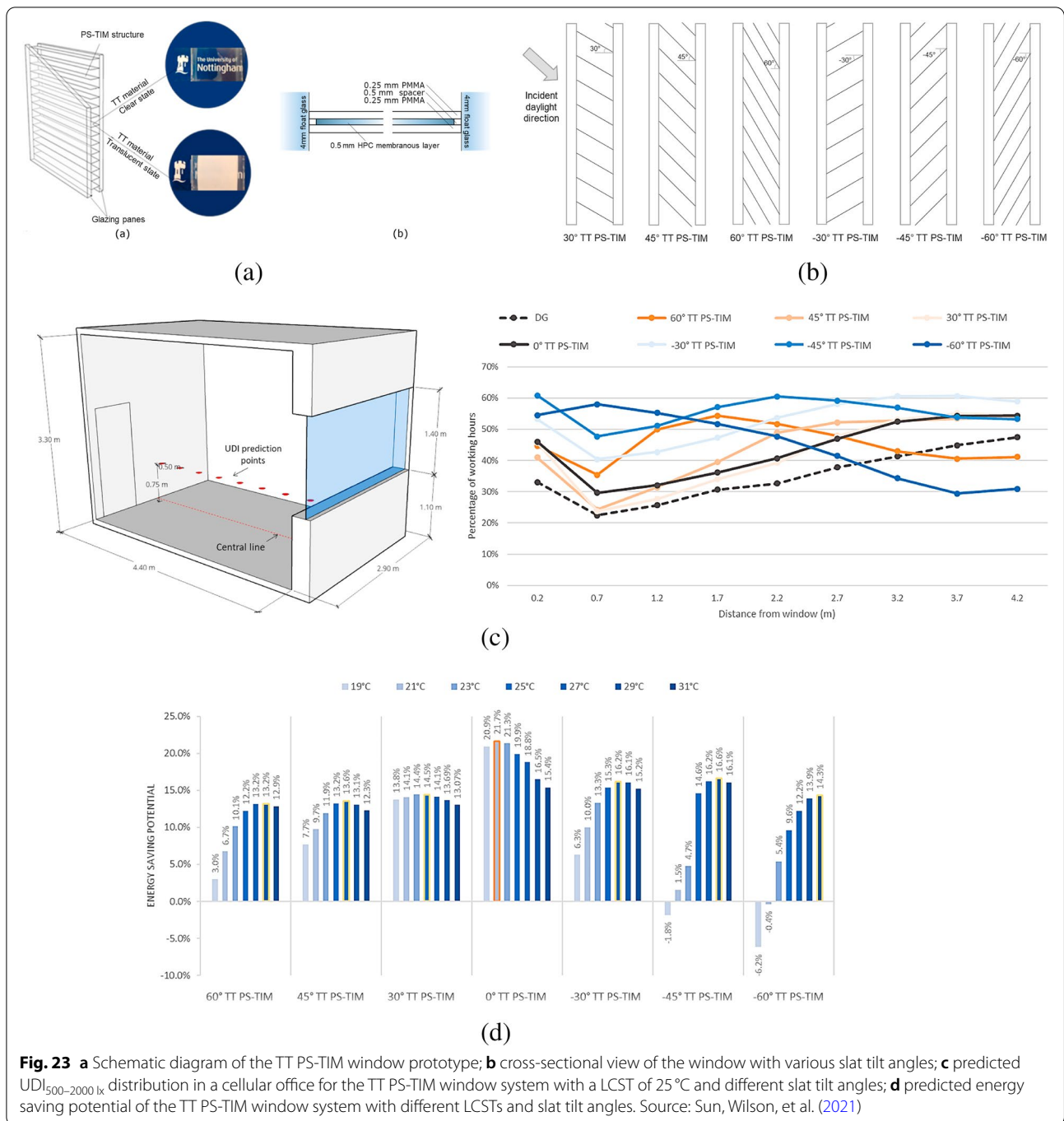
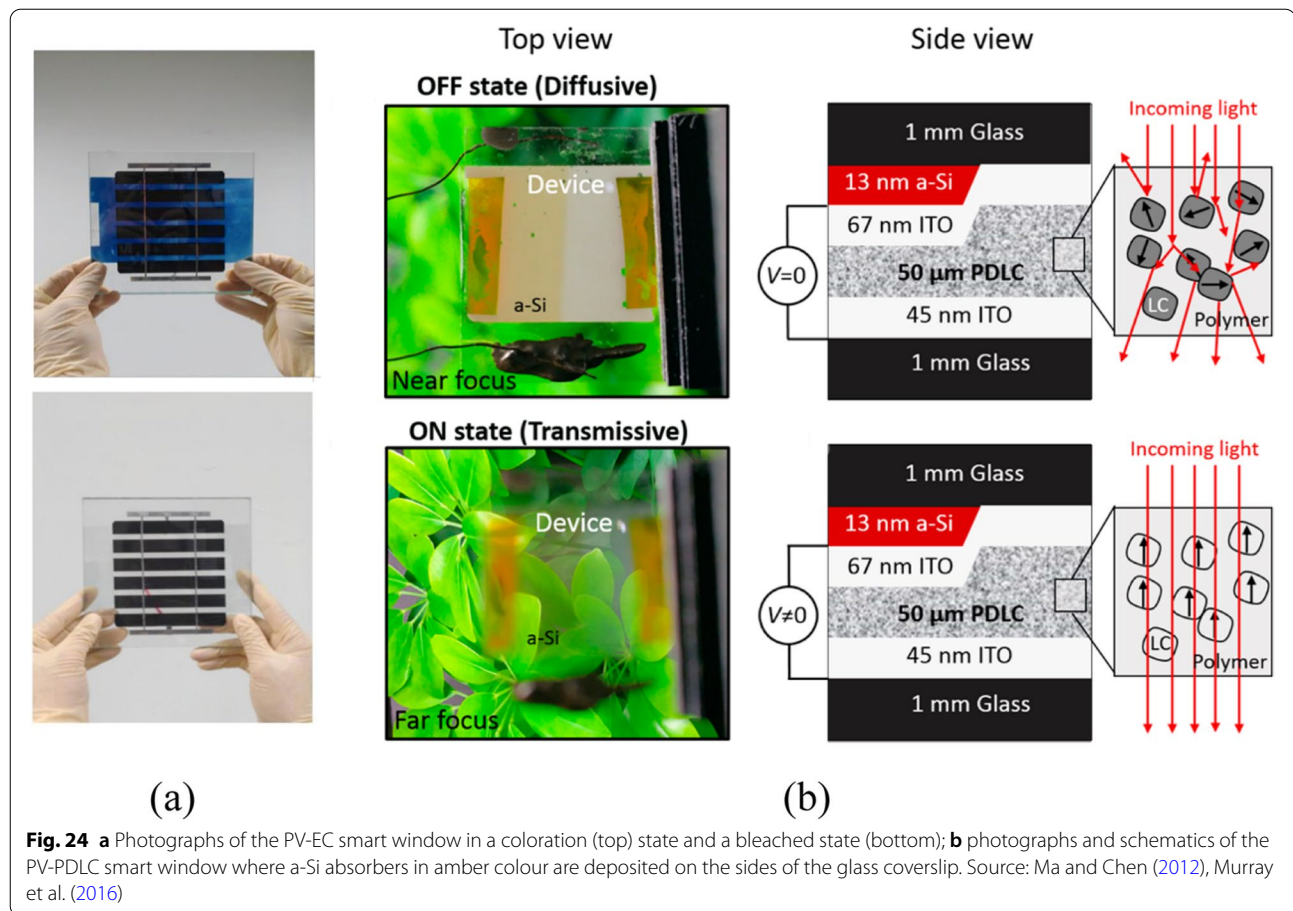


Fig. 23 **a** Schematic diagram of the TT PS-TIM window prototype; **b** cross-sectional view of the window with various slat tilt angles; **c** predicted $UDI_{500-2000\text{ lx}}$ distribution in a cellular office for the TT PS-TIM window system with a LCST of 25°C and different slat tilt angles; **d** predicted energy saving potential of the TT PS-TIM window system with different LCSTs and slat tilt angles. Source: Sun, Wilson, et al. (2021)

(c). This technology circumvents the fundamental trade-off between high τ_{vis} and good PCE that limits the widespread application of traditional semi-transparent PVs. However, due to degradation or morphological changes to the $CH_3NH_3PbI_3$ layer, the PV window had decreased electrical performance after 20 cycles.

Zhou et al. (2013) reported an electricity-generating smart window that utilised a VO_2 -based thermochromic

film to regulate the near-infrared transmittance in response to temperature change and simultaneously scatter a portion of incident light to the edge-attached poly c-Si solar cells for electricity production. Power conversion efficiencies of only up to 0.52% were realised by the light-scattering effect. Moreover, the applied VO_2 film has a transition temperature as high as 68°C, which limits the use of the window for practical applications.



Wu et al. (2016) proposed an HPC based thermotropic reflective layer for integration within a BIPV window/ façade (see Fig. 26), in order to improve both daylighting control and PV power performance. An optical model developed with the aid of a 3D ray-tracing technique was used for the system design and optical analysis. The optical efficiency and optical concentration ratio of the system were predicted to be 10% and 0.5, respectively, when the diffuse reflectivity of the thermotropic layer was set to be 50% in the model. The study opens a new route to develop a facile, cost effective, multifunctional window.

The concept of combined PV-TT smart windows has been further explored and validated by Liu and Wu (2021a, 2021b, 2021c, 2022) using sophisticated simulation models and undertaking experiments under laboratory and outdoor conditions. Smart windows with different LCSTs (between 20°C and 40°C), excellent solar energy modulations (up to 76%) and good electrical performance (up to 12% improvement in power output compared to an ordinary c-Si PV glazing) have been demonstrated. EnergyPlus simulation was conducted to predict the window's dynamic behaviour in a building environment. Figure 27 shows the adaptive control over solar heat gain and indoor

illumination level by the proposed BIPV smart window, which consists of an HPC based thermotropic hydrogel membrane (LCST = 30.5°C), front-facing c-Si PV cells and glass panes. In winter months, there is no significant solar heat gain difference between the BIPV smart window and its counterpart (with a similar window design but no thermotropic layer). In summer months, the BIPV smart window gives obviously lower solar heat gains than the reference windows. On a hot sunny day, the BIPV smart window can automatically lower its visible transparency as being heated up by intense solar radiation, which enables effective protection against the indoor visual discomfort induced by over-illumination (i.e., over 2000 lx). Nevertheless, for practical applications, problems associated with the long-term performance degradation of the BIPV smart window need to be addressed, such as hydrogel leakage or dry-out because of improper window sealing, and material deterioration due to mould growth in the hydrogel.

6 Discussion and recommendations

There is a wide range of static, dynamic, and smart glazing technologies for daylighting control and energy-saving purposes. BIPV glazing that provides effective

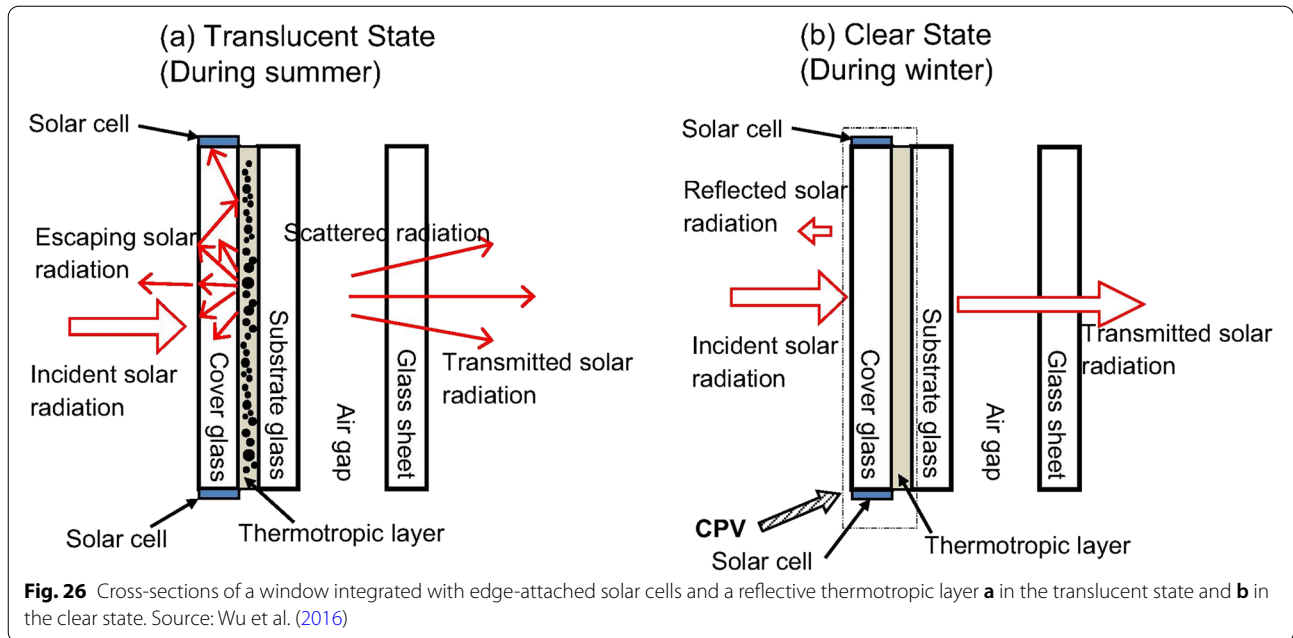


Fig. 26 Cross-sections of a window integrated with edge-attached solar cells and a reflective thermotropic layer **a** in the translucent state and **b** in the clear state. Source: Wu et al. (2016)

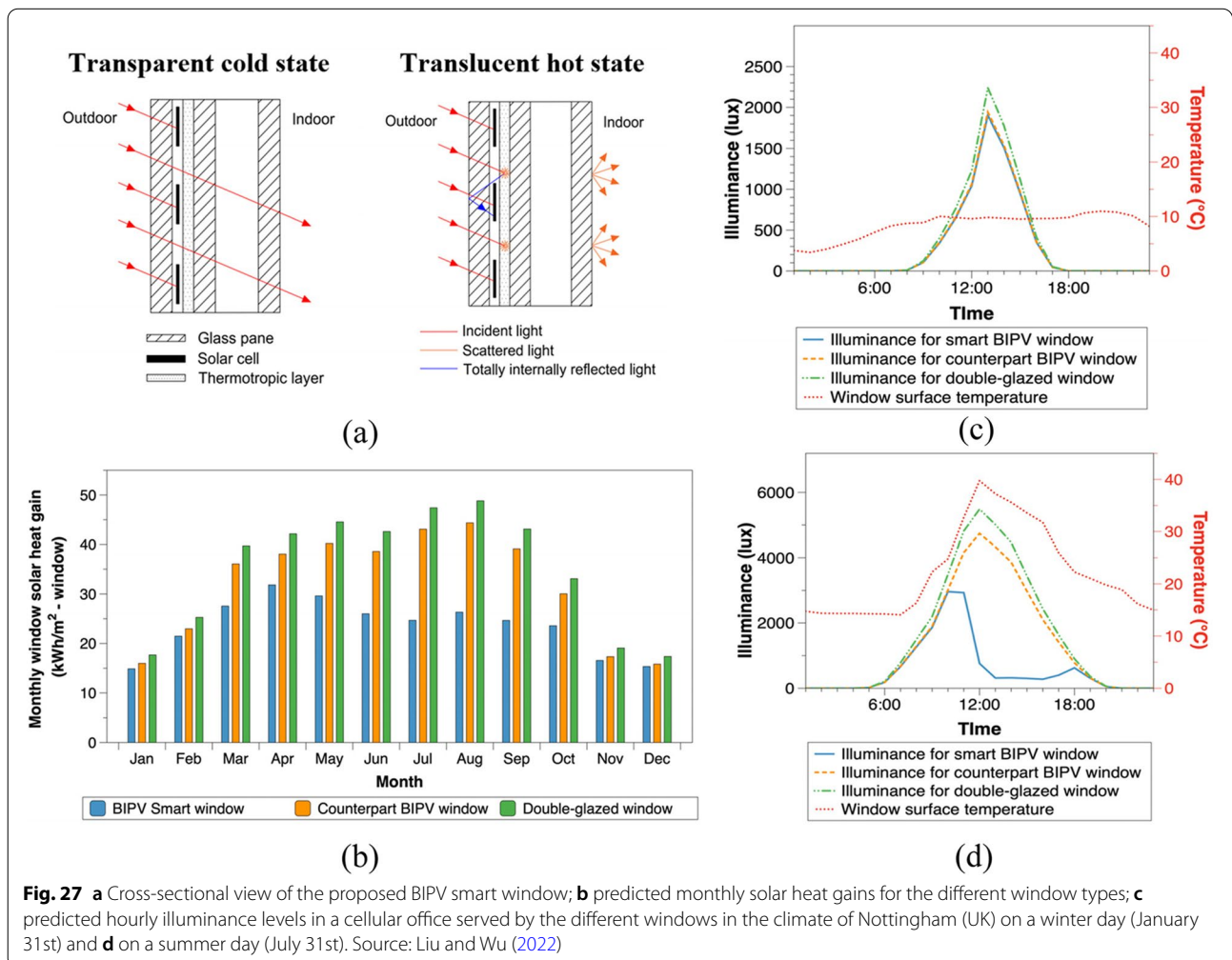


Fig. 27 **a** Cross-sectional view of the proposed BIPV smart window; **b** predicted monthly solar heat gains for the different window types; **c** predicted hourly illuminance levels in a cellular office served by the different windows in the climate of Nottingham (UK) on a winter day (January 31st) and **d** on a summer day (July 31st). Source: Liu and Wu (2022)

solar shading together with on-site electricity generation occupies a pivotal position. Solar cells such as c-Si, a-Si, CdTe and DSSC find their applications in BIPV glazing, each of which has its advantages and disadvantages (see Table 2). Of these, opaque c-Si solar cells are a well-established technology with high PCE (up to 25%), long operational lifetime (30 years) and short energy payback time (EPBT) (4 years) (Ogbomo et al., 2017), which are suitable for commercial applications. However, when designing this kind of PV glazing, a compromise should be made between high transparency (using

a low coverage area of c-Si solar cells) and high electricity output (using a high coverage area of c-Si solar cells). Integrating PV glazing with solar concentrator technology can reduce the PV cell coverage area for good daylighting without sacrificing the electricity output. The solutions offered so far include CPV glazing modules based on Flat-plate Static Concentrators (FPSCs) and Dielectric based Compound Parabolic Concentrators (DiCPCs) (see Table 2). A FPSC is typically made of one or multiple transparent waveguides (e.g., glass or PMMA plates) coated or doped with materials that exhibit

Table 2 Performance and challenges of BIPV and BICPV glazing technologies

		Features	Challenges	Effect on building performance
BIPV glazing system	c-Si	<ul style="list-style-type: none"> * Well-developed PV technology * High power conversion efficiency of solar cell and BIPV module 	<ul style="list-style-type: none"> * Opaque and thick solar cell * PCE is susceptible to PV operating temperature and shading 	<ul style="list-style-type: none"> * Solar heat gain and daylighting reductions * Inhomogeneous daylighting for the interior space
	a-Si	<ul style="list-style-type: none"> * Semi-transparent, thin, lightweight, bendable * Low cost in large scale production * Better heat resistance than c-Si * Long operational lifetime 	<ul style="list-style-type: none"> * Low power conversion efficiency * Increasing the PCE would sacrifice the cell transparency 	<ul style="list-style-type: none"> * Lower cooling loads in summer but higher heating loads in winter * Better uniformity of illumination in the indoor space than c-Si BIPV glazing * Auxiliary shading devices are needed to eliminate glare
	CdTe	<ul style="list-style-type: none"> * High PCE, low generation cost and low energy payback time * Good performance at elevated temperature * Fast deposition process 	<ul style="list-style-type: none"> * Detrimental effects on human health and environment * Dark colours 	
	DSSC	<ul style="list-style-type: none"> * Various transparencies & colours * Good performance in variable lighting conditions * Simple manufacture and low cost 	<ul style="list-style-type: none"> * Low power conversion efficiency * Chemical degradation * Electrolyte leakage 	
	PSC	<ul style="list-style-type: none"> * Ease of bandgap tuning * High power conversion efficiency * Low-cost material processing and deposition 	<ul style="list-style-type: none"> * Unsatisfactory operational stability * Toxicity 	
BICPV glazing system	Luminescent solar concentrator (LSC)	<ul style="list-style-type: none"> * Various degrees of transparency and colour * Large acceptance angle * Simple manufacture and low cost 	<ul style="list-style-type: none"> * High optical loss due to light escaping, reabsorption, etc. * Low optical efficiency 	
	Lambertian rear reflector	<ul style="list-style-type: none"> * Light-scattering effect * More uniform irradiation on solar cell than BICPV with V-grooved rear reflector, CPC, etc. 	<ul style="list-style-type: none"> * High reflectance but low transparency, potentially not suitable for glazing application. 	<ul style="list-style-type: none"> * Glare reduction * Poor passive solar heating and daylighting
	Compound parabolic concentrator (CPC)	<ul style="list-style-type: none"> * High optical efficiency and optical concentration ratio 	<ul style="list-style-type: none"> * Non-uniform solar irradiation and temperature distribution on PV cell * Cell deterioration due to hot spot * Non-planar and bulky structure 	<ul style="list-style-type: none"> * The coverage area of solar cells in BIPV glazing is reduced without compromising the power output * The concentrating optics may distort the view out of building

strong scattering (e.g., TiO_2 particles) or luminescent properties (e.g., fluorescent dyes or quantum dots). c-Si solar cells are optically attached to the edges or bottom of the waveguides of the FPSC to collect the photons incident directly as well as those being trapped in the waveguides by Total Internal Reflection (TIR). A major shortcoming associated with FPSCs for glazing applications is that they cannot have both high transparency (for daylighting and viewing) and high optical efficiency (for power generation). Compared with FPSCs, CPCs made of transparent dielectric materials (e.g., PMMA and polyurethane) show greater potential to overcome the optical efficiency limitation while preserving acceptable visibility. For example, the optical efficiency of a CPV glazing module based on 3D Crossed Compound Parabolic Concentrators (3DCCPCs) can reach up to 73% and its power output is 2.65 times higher than its counterpart without 3DCCPCs at normal light incidence (Baig, Sellami, et al., 2014). Despite excellent PV power performance, BICPV glazing units incorporating DiCPCs have some inherent shortcomings, such as degradation in cell performance due to hot-spot formation, visual distortion, and bulky structure.

Another challenge faced by traditional BIPV glazing is the lack of dynamic control over daylight and solar heat transmission to cope with variations in weather conditions and seasonal heating/cooling demands of buildings. In view of this situation, a new generation of PV glazing technologies, which combines PV glazing modules with optically switchable materials (e.g., electrochromic and thermochromic materials), has been developed. A detailed description of different switchable PV glazing technologies can be found in our previous publication (Castillo et al., 2022). This review paper focuses on the potential use of thermo-responsive polymer materials in PV glazing which has not been yet fully explored. As a representative example, thermotropic hydrogels (e.g., PNIPAm, HPC and HPMC) have been thoroughly evaluated through spectroscopic measurement and building energy simulation. They have been proven to be effective in the adaptive control of visible and near-infrared light transmission through windows under varying ambient conditions, which can help in reducing building energy consumption and occupant discomfort. When applied in PV glazing, thermotropic hydrogel can improve the PV power performance in addition to the control of solar heat gain and indoor illuminance. This is because with the phase transition of thermotropic hydrogel from clear to translucent (or light-scattering), the TT-PV glazing turns into a CPV module with higher electricity output.

On the other hand, the phase transition cannot be actively controlled, and only occurs when the PV-TT glazing is heated or cooled to a threshold temperature

(LCST) by the changes of ambient conditions such as solar radiation, air temperature and wind speed. On some occasions, occupants may have to endure a period of visual/thermal discomfort before the phase transition can occur. For example, on a cool, bright day, the PV-TT glazing may have low temperatures and stay transparent, failing to provide immediate protection against glare/overheating discomfort of occupants; on a hot, cloudy day, the PV-TT glazing may maintain a translucent state, and occupants may feel uncomfortable in the dim room and so turn on electric lamps. To address this issue, a transparent heating/cooling device such as invisible mesh-based electrode (Kiruthika & Kulkarni, 2017) or micro-channel (Heiz et al., 2017) can be embedded in the TT hydrogel layer of the PV-TT glazing for precise temperature control and fast switching. Future work is also recommended to develop low-heat-loss switchable PV glazing systems for use in cold climates, for example, combination of PV-TT glazing with vacuum technology.

7 Conclusions

The increasing attention to energy savings and comfort enhancement in buildings has led to the development of innovative, high-performance glazing technologies. This paper outlines the different types of glazing that can generate electricity (e.g., photovoltaic glazing), intelligently regulate daylight transmission (e.g., thermotropic smart glazing) or encompass both functions (e.g., combined PV-TT glazing). The aim of this paper is to provide the reader with an understanding of their development process, advantages and limitations, and challenges on the road ahead. PV glazing can convert solar energy into electricity, showing great potential in improving building energy efficiency and reducing carbon footprint. However, low electricity output is one of the major bottlenecks in the practical application of PV glazing. Combining PV glazing with solar concentrating technology is a feasible solution to enhance the electricity output. Semi-transparent solar concentrators such as Luminescent Solar Concentrators (LSCs) and Dielectric based Compound Parabolic Concentrators (DiCPCs) can collect ambient light from a wide range of angles and concentrate the captured light onto glazing integrated PV cells, while allowing the unabsorbed light into buildings for space heating and illumination purposes. In general, a compromise should be made between efficient solar concentration and high transparency of CPV glazing modules. Future CPV glazing designs can consider using smart materials with switchable optical properties (such as thermotropic hydrogels) as the concentrating optics to circumvent the trade-off. It is hoped that this paper will inspire future research to make energy efficient smart windows a practical solution and will serve as a step towards the development of low carbon and energy efficient buildings.

Nomenclature

3DCCPC: 3D crossed compound Parabolic concentrator; ACPC: Asymmetric compound parabolic concentrator; AM1.5: Air mass 1.5; a-Si: Amorphous silicon; BIPV: Building integrated photovoltaic; BICPV: Building integrated concentrating photovoltaic; CCT: Correlated colour temperature; CdTe: Cadmium telluride; CPC: Compound parabolic concentrator; CPV: Concentrating photovoltaic; CRI: Colour rendering index; c-Si: Crystalline silicon; DGP: Daylight glare probability; DiCPC: Dielectric based compound parabolic concentrator; DSSC: Dye-sensitised solar cell; EC: Electrochromic; EPBT: Energy payback time; EVA: Ethylene-vinyl acetate; FPSC: Flat plate static concentrator; HEC: Hydroxyethyl cellulose; HPC: Hydroxypropyl cellulose; HPMC: Hydroxypropyl methyl cellulose; ITO: Indium tin oxide; TT-IGU: Thermotropic insulation glazing unit; LCST: Lower critical saturation temperature; Low-E: Low emissivity; LSC: Luminescent solar concentrator; NaCl: Sodium chloride; n-ZEB: Near zero energy building; NIR: Near-infrared; PCE: Power conversion efficiency; PCM: Phase change material; PDLC: Polymer dispersed liquid crystals; PDMS: Polydimethylsiloxane; PECVD: Plasma-enhanced chemical vapour deposition; PMMA: Polymethylmethacrylate; PSC: Perovskite solar cell; PNIPAm: Poly(N-isopropylacrylamide); PNIPAm-AEMA: Poly(N-isopropylacrylamide)-2-aminoethylmethacrylate hydrochloride; PVB: Polyvinyl butyral; SHGC: Solar heat gain coefficient; SPD: Suspended particle device; TC: Thermochromic; TIR: Total internal reflection; TiO₂: Titanium dioxide; TT: Thermotropic; TT-PS-TIM: Thermotropic parallel slat transparent insulation material; UDI: Useful daylight illuminance; UV: Ultraviolet; WWR: Window-to-wall ratio; WO₃: Tungsten oxide; τ_{vis} : Visible light transmittance; C_g : Optical concentration ratio; η_o : Optical efficiency; ΔT_{lum} : Luminous transmittance modulation; ΔT_{IR} : Near-infrared transmittance modulation; ΔT_{sol} : Solar transmittance modulation; λ : Wavelength; r: Particle's radius.

Acknowledgements

This work was supported by the Faculty of Engineering, University of Nottingham and the China Scholarship Council through a joint PhD studentship awarded to Xiao Liu. This work was also supported by the Engineering and Physical Sciences Research Council, UK [grant number EP/S030786/1].

Authors' contributions

Xiao Liu: Writing - original draft, Literature search, Data analysis. Yupeng Wu: Writing - reviewing & editing, Funding acquisition, Supervision. The author(s) read and approved the final manuscript.

Availability of data and materials

The authors declare that all data generated or analysed during this study are available in this published article.

Declarations

Competing interests

The authors declare that they have no known competing financial interests or personal relationships that could have appeared to influence the work reported in this paper.

Received: 7 May 2022 Accepted: 13 July 2022

Published online: 03 August 2022

References

- Aburas, M., Soebarto, V., Williamson, T., Liang, R., Ebendorff-Heidepriem, H., & Wu, Y. (2019). Thermochromic smart window technologies for building application: A review. *Applied Energy*, *255*, 113522.
- Abu-Bakar, S. H., Muhammad-Sukki, F., Freier, D., Ramirez-Iniguez, R., Mallick, T. K., Munir, A. B., Yasin, S. H. M., Mas'Ud, A. A., & Yunus, N. M. (2015). Optimisation of the performance of a novel rotationally asymmetrical optical concentrator design for building integrated photovoltaic system. *Energy*, *90*, 1033–1045.
- Aguilar, J., Xaman, J., Álvarez, G., Hernández-Pérez, I., & López-Mata, C. (2015). Thermal performance of a double pane window using glazing available on the Mexican market. *Renewable Energy*, *81*, 785–794.
- Allen, K., Connelly, K., Rutherford, P., & Wu, Y. (2017). Smart windows—Dynamic control of building energy performance. *Energy and Buildings*, *139*, 535–546.
- Alrashidi, H., Ghosh, A., Issa, W., Sellami, N., Mallick, T. K., & Sundaram, S. (2019). Evaluation of solar factor using spectral analysis for CdTe photovoltaic glazing. *Materials Letters*, *237*, 332–335.
- Alrashidi, H., Ghosh, A., Issa, W., Sellami, N., Mallick, T. K., & Sundaram, S. (2020). Thermal performance of semitransparent CdTe BIPV window at temperate climate. *Solar Energy*, *195*, 536–543.
- Andreani, L. C., Bozzola, A., Kowalczewski, P., Liscidini, M., & Redorici, L. (2019). Silicon solar cells: Toward the efficiency limits. *Advances in Physics: X*, *4*, 1548305.
- Arici, M., & Kan, M. (2015). An investigation of flow and conjugate heat transfer in multiple pane windows with respect to gap width, emissivity and gas filling. *Renewable Energy*, *75*, 249–256.
- Arici, M., Karabay, H., & Kan, M. (2015). Flow and heat transfer in double, triple and quadruple pane windows. *Energy and Buildings*, *86*, 394–402.
- Aydin, E., Allen, T. G., De Bastiani, M., Xu, L., Ávila, J., Salvador, M., Van Kerschaver, E., & De Wolf, S. (2020). Interplay between temperature and bandgap energies on the outdoor performance of perovskite/silicon tandem solar cells. *Nature Energy*, *5*, 851–859.
- Baetens, R., Jelle, B. P., & Gustavsen, A. (2010). Properties, requirements and possibilities of smart windows for dynamic daylight and solar energy control in buildings: A state-of-the-art review. *Solar Energy Materials and Solar Cells*, *94*, 87–105.
- Baig, H., Sarmah, N., Chemisana, D., Rosell, J., & Mallick, T. K. (2014). Enhancing performance of a linear dielectric based concentrating photovoltaic system using a reflective film along the edge. *Energy*, *73*, 177–191.
- Baig, H., Sarmah, N., Heasman, K. C., & Mallick, T. K. (2013). Numerical modelling and experimental validation of a low concentrating photovoltaic system. *Solar Energy Materials and Solar Cells*, *113*, 201–219.
- Baig, H., Sellami, N., Chemisana, D., Rosell, J., & Mallick, T. K. (2014). Performance analysis of a dielectric based 3D building integrated concentrating photovoltaic system. *Solar Energy*, *103*, 525–540.
- Baig, H., Sellami, N., & Mallick, T. K. (2015). Trapping light escaping from the edges of the optical element in a concentrating photovoltaic system. *Energy Conversion and Management*, *90*, 238–246.
- Bergren, M. R., Makarov, N. S., Ramasamy, K., Jackson, A., Guglielmetti, R., & McDaniel, H. (2018). High-performance CuInS₂ quantum dot laminated glass luminescent solar concentrators for windows. *ACS Energy Letters*, *3*, 520–525.
- Bhandari, S., Ghosh, A., Roy, A., Mallick, T. K., & Sundaram, S. (2022). Compelling temperature behaviour of carbon-perovskite solar cell for fenestration at various climates. *Chemical Engineering Journal Advances*, *10*, 100267.
- Cannavale, A., Hörantner, M., Eperon, G. E., Snaith, H. J., Fiorito, F., Ayr, U., & Martellotta, F. (2017). Building integration of semitransparent perovskite-based solar cells: Energy performance and visual comfort assessment. *Applied Energy*, *194*, 94–107.
- Cannavale, A., Ierardi, L., Hörantner, M., Eperon, G. E., Snaith, H. J., Ayr, U., & Martellotta, F. (2017). Improving energy and visual performance in offices using building integrated perovskite-based solar cells: A case study in southern Italy. *Applied Energy*, *205*, 834–846.
- Cao, D., Xu, C., Lu, W., Qin, C., & Cheng, S. (2018). Sunlight-Driven Photo-Thermochromic Smart Windows. *Solar RRL*, *2*, 1700219.
- Casini, M. (2016). *Smart buildings: Advanced materials and nanotechnology to improve energy-efficiency and environmental performance*. Woodhead Publishing.
- Casini, M. (2018). Active dynamic windows for buildings: A review. *Renewable Energy*, *119*, 923–934.
- Castillo, M. S., Liu, X., Abd-Alhamid, F., Connelly, K., & Wu, Y. (2022). Intelligent windows for electricity generation: A technologies review. In *Building Simulation* (pp. 1–27). Springer.
- Chae, Y. T., Kim, J., Park, H., & Shin, B. (2014). Building energy performance evaluation of building integrated photovoltaic (BIPV) window with semi-transparent solar cells. *Applied Energy*, *129*, 217–227.
- Chemisana, D. (2011). Building integrated concentrating photovoltaics: A review. *Renewable and Sustainable Energy Reviews*, *15*, 603–611.
- Chemisana, D., Rosell, J., Riverola, A., & Lamnatou, C. (2016). Experimental performance of a Fresnel-transmission PVT concentrator for building-façade integration. *Renewable Energy*, *85*, 564–572.
- Chen, M., Zhang, W., Xie, L., Ni, Z., Wei, Q., Wang, W., & Tian, H. (2019). Experimental and numerical evaluation of the crystalline silicon PV window under the climatic conditions in Southwest China. *Energy*, *183*, 584–598.

- Chou, C.-H., Chuang, J.-K., & Chen, F.-C. (2013). High-performance flexible waveguiding photovoltaics. *Scientific reports*, 3, 2244.
- Chow, T.-T., Li, C., & Lin, Z. (2010). Innovative solar windows for cooling-demand climate. *Solar Energy Materials and Solar Cells*, 94, 212–220.
- Chung, M. H., Park, B. R., Choi, E. J., Choi, Y. J., Lee, C., Hong, J., Cho, H. U., Cho, J. H., & Moon, J. W. (2020). Performance level criteria for semi-transparent photovoltaic windows based on dye-sensitized solar cells. *Solar Energy Materials and Solar Cells*, 217, 110683.
- Connelly, K., Wu, Y., Chen, J., & Lei, Y. (2016). Design and development of a reflective membrane for a novel building integrated concentrating photovoltaic (BICPV) 'smart window' system. *Applied Energy*, 182, 331–339.
- Connelly, K., Wu, Y., Ma, X., & Lei, Y. (2017). Transmittance and reflectance studies of thermotropic material for a novel building integrated concentrating photovoltaic (BICPV) smart window system. *Energies*, 10, 1889.
- Corrado, C., Leow, S. W., Osborn, M., Chan, E., Balaban, B., & Carter, S. A. (2013). Optimization of gain and energy conversion efficiency using front-facing photovoltaic cell luminescent solar concentrator design. *Solar Energy Materials and Solar Cells*, 111, 74–81.
- Cuce, E., & Riffat, S. B. (2015). A state-of-the-art review on innovative glazing technologies. *Renewable and Sustainable Energy Reviews*, 41, 695–714.
- Cui, Y., Ke, Y., Liu, C., Chen, Z., Wang, N., Zhang, L., Zhou, Y., Wang, S., Gao, Y., & Long, Y. (2018). Thermochromic VO₂ for energy-efficient smart windows. *Joule*, 2, 1707–1746.
- Du, H., Wickramasinghe, R., & Qian, X. (2010). Effects of salt on the lower critical solution temperature of poly (N-isopropylacrylamide). *The Journal of Physical Chemistry B*, 114, 16594–16604.
- Faheem, M. B., Khan, B., Hashmi, J. Z., Baniya, A., Subhani, W., Bobba, R. S., Yildiz, A., & Qiao, Q. (2022). Insights from scalable fabrication to operational stability and industrial opportunities for perovskite solar cells and modules. *Cell Reports Physical Science*, 3, 100827.
- Favoino, F., Fiorito, F., Cannavale, A., Ranzi, G., & Overend, M. (2016). Optimal control and performance of photovoltachromic switchable glazing for building integration in temperate climates. *Applied Energy*, 178, 943–961.
- Favoino, F., Overend, M., & Jin, Q. (2015). The optimal thermo-optical properties and energy saving potential of adaptive glazing technologies. *Applied Energy*, 156, 1–15.
- Fung, T. Y., & Yang, H. (2008). Study on thermal performance of semi-transparent building-integrated photovoltaic glazings. *Energy and Buildings*, 40, 341–350.
- Gao, Y., Si, F. T., Isabella, O., Santbergen, R., Yang, G., Dong, J., Zhang, G., & Zeman, M. (2017). *Performance Optimization of Semi-Transparent Thin-Film Amorphous Silicon Solar Cells, 2017 IEEE 44th Photovoltaic Specialist Conference (PVSC)* (pp. 2605–2609). IEEE.
- Ghosh, A. (2020). Potential of building integrated and attached/applied photovoltaic (BIPV/BAPV) for adaptive less energy-hungry building's skin: A comprehensive review. *Journal of Cleaner Production*, 276, 123343.
- Ghosh, A., & Norton, B. (2018). Advances in switchable and highly insulating autonomous (self-powered) glazing systems for adaptive low energy buildings. *Renewable Energy*, 126, 1003–1031.
- Ghosh, A., Norton, B., & Duffy, A. (2017). Effect of atmospheric transmittance on performance of adaptive SPD-vacuum switchable glazing. *Solar Energy Materials and Solar Cells*, 161, 424–431.
- Ghosh, A., Selvaraj, P., Sundaram, S., & Mallick, T. K. (2018). The colour rendering index and correlated colour temperature of dye-sensitized solar cell for adaptive glazing application. *Solar Energy*, 163, 537–544.
- Ghosh, A., Sundaram, S., & Mallick, T. K. (2019). *Thermal performance analysis of BIPV-PDLC window*.
- Gladden, A., Mantell, S., & Davidson, J. (2015). Numerical evaluation of the optical properties of encapsulated phase change particles for thermotropic materials. *Journal of Thermal Science and Engineering Applications*, 7, 031002.
- Gorgolis, G., & Karamanis, D. (2016). Solar energy materials for glazing technologies. *Solar Energy Materials and Solar Cells*, 144, 559–578.
- Granqvist, C. G. (2007). Transparent conductors as solar energy materials: A panoramic review. *Solar Energy Materials and Solar Cells*, 91, 1529–1598.
- Guo, F., Chen, S., Chen, Z., Luo, H., Gao, Y., Przybilla, T., Spiecker, E., Osvet, A., Forberich, K., & Brabec, C. J. (2015). Printed smart photovoltaic window integrated with an energy-saving Thermochromic layer. *Advanced Optical Materials*, 3, 1524–1529.
- Hee, W., Alghoul, M., Bakhtyar, B., Elayeb, O., Shameri, M., Alrubaihi, M., & Sopian, K. (2015). The role of window glazing on daylighting and energy saving in buildings. *Renewable and Sustainable Energy Reviews*, 42, 323–343.
- Heiz, B. P., Pan, Z., Lautenschläger, G., Sirtl, C., Kraus, M., & Wondraczek, L. (2017). Ultrathin fluidic laminates for large-area façade integration and smart windows. *Advanced Science*, 4, 1600362.
- Hezel, R. (2003). Novel applications of bifacial solar cells. *Progress in Photovoltaics: Research and Applications*, 11, 549–556.
- Husain, A. A., Hasan, W. Z. W., Shafie, S., Hamidon, M. N., & Pandey, S. S. (2018). A review of transparent solar photovoltaic technologies. *Renewable and Sustainable Energy Reviews*, 94, 779–791.
- Jelle, B. P., Breivik, C., & Røkenes, H. D. (2012). Building integrated photovoltaic products: A state-of-the-art review and future research opportunities. *Solar Energy Materials and Solar Cells*, 100, 69–96.
- Jelle, B. P., Kalnæs, S. E., & Gao, T. (2015). Low-emissivity materials for building applications: A state-of-the-art review and future research perspectives. *Energy and Buildings*, 96, 329–356.
- Jiang, T., Zhao, X., Yin, X., Yang, R., & Tan, G. (2021). Dynamically adaptive window design with thermo-responsive hydrogel for energy efficiency. *Applied Energy*, 287, 116573.
- Jin, X., Kang, H., Liu, R., & Huang, Y. (2013). Regulation of the thermal sensitivity of hydroxypropyl cellulose by poly (N-isopropylacrylamide) side chains. *Carbohydrate Polymers*, 95, 155–160.
- Kamalisarvestani, M., Saidur, R., Mekhilef, S., & Javadi, F. (2013). Performance, materials and coating technologies of thermochromic thin films on smart windows. *Renewable and Sustainable Energy Reviews*, 26, 353–364.
- Karabay, H., & Arıcı, M. (2012). Multiple pane window applications in various climatic regions of Turkey. *Energy and Buildings*, 45, 67–71.
- Kasezawa, T., Horimai, H., Tabuchi, H., & Shimura, T. (2016). Holographic window for solar power generation. *Optical Review*, 23, 997–1003.
- Kerrouche, A., Hardy, D., Ross, D., & Richards, B. (2014a). Luminescent solar concentrators: From experimental validation of 3D ray-tracing simulations to coloured stained-glass windows for BIPV. *Solar Energy Materials and Solar Cells*, 122, 99–106.
- Kerrouche, A., Hardy, D. A., Ross, D., & Richards, B. S. (2014b). Luminescent solar concentrators: From experimental validation of 3D ray-tracing simulations to coloured stained-glass windows for BIPV. *Solar Energy Materials and Solar Cells*, 122, 99–106.
- Kim, G.-H., & Kim, D. S. (2021). Development of perovskite solar cells with > 25% conversion efficiency. *Joule*, 5, 1033–1035.
- Kim, J. M., & Dutta, P. S. (2012). Optical efficiency–concentration ratio trade-off for a flat panel photovoltaic system with diffuser type concentrator. *Solar Energy Materials and Solar Cells*, 103, 35–40.
- Kim, N., Lee, S., Zhao, X. G., Kim, D., Oh, C., & Kang, H. (2016). Reflection and durability study of different types of backsheets and their impact on c-Si PV module performance. *Solar Energy Materials and Solar Cells*, 146, 91–98.
- Kiruthika, S., & Kulkarni, G. (2017). Energy efficient hydrogel based smart windows with low cost transparent conducting electrodes. *Solar Energy Materials and Solar Cells*, 163, 231–236.
- Kwon, H. K., Lee, K. T., Hur, K., Moon, S. H., Quasim, M. M., Wilkinson, T. D., Han, J. Y., Ko, H., Han, I. K., & Park, B. (2015). Optically switchable smart windows with integrated photovoltaic devices. *Advanced Energy Materials*, 5, 1401347.
- Lanzalaco, S., & Armelin, E. (2017). Poly (n-isopropylacrylamide) and copolymers: A review on recent progresses in biomedical applications. *Gels*, 3, 36.
- Lee, H. M., & Yoon, J. H. (2018). Power performance analysis of a transparent DSSC BIPV window based on 2 year measurement data in a full-scale mock-up. *Applied Energy*, 225, 1013–1021.
- Leftheriotis, G., & Yianoulis, P. (2012). 3.10 - Glazings and coatings. In *Comprehensive renewable energy*. Elsevier.
- Leow, S. W., Corrado, C., Osborn, M., & Carter, S. A. (2013). Monte Carlo ray-tracing simulations of luminescent solar concentrators for building integrated photovoltaics. In *High and Low Concentrator Systems for Solar Electric Applications VIII*, 8821, 882103.
- Leow, S. W., Corrado, C., Osborn, M., Isaacson, M., Alers, G., & Carter, S. A. (2013). Analyzing luminescent solar concentrators with front-facing photovoltaic cells using weighted Monte Carlo ray tracing. *Journal of Applied Physics*, 113, 214510.

- Li, C., Chen, M., Zhang, L., Shen, W., Liang, X., Wang, X., & Yang, H. (2020). An electrically light-transmittance-switchable film with a low driving voltage based on liquid crystal/polymer composites. *Liquid Crystals*, *47*, 106–113.
- Li, H., & Zhang, W. (2020). Perovskite tandem solar cells: From fundamentals to commercial deployment. *Chemical Reviews*, *120*, 9835–9950.
- Li, X.-H., Liu, C., Feng, S.-P., & Fang, N. X. (2019). Broadband light management with thermochromic hydrogel microparticles for smart windows. *Joule*, *3*, 290–302.
- Liao, W., & Xu, S. (2015). Energy performance comparison among see-through amorphous-silicon PV (photovoltaic) glazings and traditional glazings under different architectural conditions in China. *Energy*, *83*, 267–275.
- Lin, J., Lai, M., Dou, L., Kley, C. S., Chen, H., Peng, F., Sun, J., Lu, D., Hawks, S. A., & Xie, C. (2018). Thermochromic halide perovskite solar cells. *Nature Materials*, *17*, 261–267.
- Liu, D., Sun, Y., Wilson, R., & Wu, Y. (2020). Comprehensive evaluation of window-integrated semi-transparent PV for building daylight performance. *Renewable Energy*, *145*, 1399–1411.
- Liu, D., Yang, C., & Lunt, R. R. (2018). Halide perovskites for selective ultraviolet-harvesting transparent photovoltaics. *Joule*, *2*, 1827–1837.
- Liu, X., & Wu, Y. (2021a). Design, development and characterisation of a building integrated concentrating photovoltaic (BICPV) smart window system. *Solar Energy*, *220*, 722–734.
- Liu, X., & Wu, Y. (2021b). Experimental characterisation of a smart glazing with tuneable transparency, light scattering ability and electricity generation function. *Applied Energy*, *303*, 117521.
- Liu, X., & Wu, Y. (2021c). Monte-Carlo optical model coupled with inverse adding-doubling for building integrated photovoltaic smart window design and characterisation. *Solar Energy Materials and Solar Cells*, *223*, 110972.
- Liu, X., & Wu, Y. (2022). Numerical evaluation of an optically switchable photovoltaic glazing system for passive daylighting control and energy-efficient building design. *Building and Environment*, *219*, 109170.
- Liu, X., Wu, Y., Hou, X., & Liu, H. (2017). Investigation of the optical performance of a novel planar static PV concentrator with Lambertian rear reflectors. *Buildings*, *7*, 88.
- Luceño-Sánchez, J. A., Díez-Pascual, A. M., & Peña Capilla, R. (2019). Materials for photovoltaics: State of art and recent developments. *International Journal of Molecular Sciences*, *20*, 976.
- Ma, R.-H., & Chen, Y.-C. (2012). BIPV-powered smart windows utilizing photovoltaic and electrochromic devices. *Sensors*, *12*, 359–372.
- Maierov, V. (2020). Optical properties of Thermotropic hydrogels (a review). *Optics and Spectroscopy*, *128*, 367–386.
- Mallik, T. K., & Eames, P. C. (2007). Design and fabrication of low concentrating second generation PRIDE concentrator. *Solar Energy Materials and Solar Cells*, *91*, 597–608.
- Meillaud, F., Boccard, M., Bugnon, G., Despeisse, M., Hänni, S., Haug, F.-J., Persoz, J., Schüttauf, J.-W., Stuckelberger, M., & Ballif, C. (2015). Recent advances and remaining challenges in thin-film silicon photovoltaic technology. *Materials Today*, *18*, 378–384.
- Miyazaki, T., Akisawa, A., & Kashiwagi, T. (2005). Energy savings of office buildings by the use of semi-transparent solar cells for windows. *Renewable Energy*, *30*, 281–304.
- Mizutani, M., Satoh, K., & Kamigaito, M. (2011). Degradable poly (N-isopropylacrylamide) with tunable thermosensitivity by simultaneous chain-and step-growth radical polymerization. *Macromolecules*, *44*, 2382–2386.
- Morimoto, M., & Maruyama, T. (2005). Static solar concentrator with vertical flat plate photovoltaic cells and switchable white/transparent bottom plate. *Solar Energy Materials and Solar Cells*, *87*, 299–309.
- Muehling, O., Seebboth, A., Haeusler, T., Ruhmann, R., Potechius, E., & Vetter, R. (2009). Variable solar control using thermotropic core/shell particles. *Solar Energy Materials and Solar Cells*, *93*, 1510–1517.
- Murray, J., Ma, D., & Munday, J. N. (2016). Electrically controllable light trapping for self-powered switchable solar windows. *ACS Photonics*, *4*, 1–7.
- National Renewable Energy Laboratory. 2022. Best Research-Cell Efficiencies Chart. Available: <https://www.nrel.gov/pv/cell-efficiency.html> [Accessed 15 June 2022].
- Nishio, Y., Chiba, R., Miyashita, Y., Oshima, K., Miyajima, T., Kimura, N., & Suzuki, H. (2002). Salt addition effects on mesophase structure and optical properties of aqueous hydroxypropyl cellulose solutions. *Polymer Journal*, *34*, 149–157.
- Nitz, P., & Hartwig, H. (2005). Solar control with thermotropic layers. *Solar Energy*, *79*, 573–582.
- Nun, N., Hinrichs, S., Schroer, M. A., Sheyfer, D., Grübel, G., & Fischer, B. (2017). Tuning the size of thermoresponsive poly (N-isopropyl acrylamide) grafted silica microgels. *Gels*, *3*, 34.
- Ogbomo, O. O., Amalu, E. H., Ekere, N., & Olagbegi, P. (2017). A review of photovoltaic module technologies for increased performance in tropical climate. *Renewable and Sustainable Energy Reviews*, *75*, 1225–1238.
- Park, K., Kang, G., Kim, H., Yu, G., & Kim, J. (2010). Analysis of thermal and electrical performance of semi-transparent photovoltaic (PV) module. *Energy*, *35*, 2681–2687.
- Paul, D. I. (2011). *Characterisation of solar concentrating systems for photovoltaics and their impact on performance*. University of Ulster.
- Peng, J., Curcija, D. C., Lu, L., Selkowitz, S. E., Yang, H., & Zhang, W. (2016). Numerical investigation of the energy saving potential of a semi-transparent photovoltaic double-skin facade in a cool-summer Mediterranean climate. *Applied Energy*, *165*, 345–356.
- Peng, J., Curcija, D. C., Thanachareonkit, A., Lee, E. S., Goudey, H., & Selkowitz, S. E. (2019). Study on the overall energy performance of a novel c-Si based semitransparent solar photovoltaic window. *Applied Energy*, *242*, 854–872.
- Piccolo, A., & Simone, F. (2015). Performance requirements for electrochromic smart window. *Journal of Building Engineering*, *3*, 94–103.
- Radwan, A., Katsura, T., Memon, S., Serageldin, A. A., Nakamura, M., & Nagano, K. (2020). Thermal and electrical performances of semi-transparent photovoltaic glazing integrated with translucent vacuum insulation panel and vacuum glazing. *Energy Conversion and Management*, *215*, 112920.
- Ramirez-Iniguez, R., Deciga-Gusi, J., Freier, D., Abu-Bakar, S. H., & Muhammad-Sukki, F. (2017). Experimental evaluation of a solar window incorporating rotationally asymmetrical compound parabolic concentrators (RACPC). *Energy Procedia*, *130*, 102–107.
- Resch, K., & Wallner, G. M. (2009). Thermotropic layers for flat-plate collectors—A review of various concepts for overheating protection with polymeric materials. *Solar Energy Materials and Solar Cells*, *93*, 119–128.
- Rezaei, S. D., Shannigrahi, S., & Ramakrishna, S. (2017). A review of conventional, advanced, and smart glazing technologies and materials for improving indoor environment. *Solar Energy Materials and Solar Cells*, *159*, 26–51.
- Rho, W.-Y., Jeon, H., Kim, H.-S., Chung, W.-J., Suh, J. S., & Jun, B.-H. (2015). Recent progress in dye-sensitized solar cells for improving efficiency: TiO₂ nanotube arrays in active layer. *Journal of Nanomaterials*, *2015*, 247689.
- Roy, A., Ghosh, A., Bhandari, S., Selvaraj, P., Sundaram, S., & Mallick, T. K. (2019). Color comfort evaluation of dye-sensitized solar cell (DSSC) based building-integrated photovoltaic (BIPV) glazing after 2 years of ambient exposure. *The Journal of Physical Chemistry C*, *123*, 23834–23837.
- Sabry, M. (2016). Prismatic TIR (total internal reflection) low-concentration PV (photovoltaics)-integrated façade for low latitudes. *Energy*, *107*, 473–481.
- Sarmah, N., & Mallick, T. K. (2015). Design, fabrication and outdoor performance analysis of a low concentrating photovoltaic system. *Solar Energy*, *112*, 361–372.
- Sarmah, N., Richards, B. S., & Mallick, T. K. (2014). Design, development and indoor performance analysis of a low concentrating dielectric photovoltaic module. *Solar Energy*, *103*, 390–401.
- Schneider, J., & Seebboth, A. (2001). Natural thermotropic materials for solar switching glazing. *Materialwissenschaft und Werkstofftechnik*, *32*, 231–237.
- Seebboth, A., Ruhmann, R., & Muehling, O. (2010). Thermotropic and thermochromic polymer based materials for adaptive solar control. *Materials*, *3*, 5143–5168.
- Seebboth, A., Schneider, J., & Patzak, A. (2000). Materials for intelligent sun projecting glazing. *Solar Energy Materials and Solar Cells*, *60*, 263–277.
- Sellami, N., & Mallick, T. K. (2013). Optical efficiency study of PV crossed compound parabolic concentrator. *Applied Energy*, *102*, 868–876.
- Selvaraj, P., Ghosh, A., Mallick, T. K., & Sundaram, S. (2019). Investigation of semi-transparent dye-sensitized solar cells for fenestration integration. *Renewable Energy*, *141*, 516–525.
- Shanks, K., Knowles, A., Brierley, A., Baig, H., Orr, H., Sun, Y., Wu, Y., Sundaram, S., & Mallick, T. (2019). An experimental analysis of the optical, thermal and power to weight performance of plastic and glass optics with AR coatings for embedded CPV windows. *Solar Energy Materials and Solar Cells*, *200*, 110027.

- Shanks, K., Senthilarasu, S., & Mallick, T. K. (2016). Optics for concentrating photovoltaics: Trends, limits and opportunities for materials and design. *Renewable and Sustainable Energy Reviews*, *60*, 394–407.
- Sharaf, O. Z., & Orhan, M. F. (2015). Concentrated photovoltaic thermal (CPVT) solar collector systems: Part I—Fundamentals, design considerations and current technologies. *Renewable and Sustainable Energy Reviews*, *50*, 1500–1565.
- Sharma, K., Sharma, V., & Sharma, S. (2018). Dye-sensitized solar cells: Fundamentals and current status. *Nanoscale Research Letters*, *13*, 381.
- Sharma, S., Tahir, A., Reddy, K., & Mallick, T. K. (2016). Performance enhancement of a building-integrated concentrating photovoltaic system using phase change material. *Solar Energy Materials and Solar Cells*, *149*, 29–39.
- Skandalos, N., & Karamanis, D. (2015). PV glazing technologies. *Renewable and Sustainable Energy Reviews*, *49*, 306–322.
- Skandalos, N., & Karamanis, D. (2016). Investigation of thermal performance of semi-transparent PV technologies. *Energy and Buildings*, *124*, 19–34.
- Smestad, G., & Hamill, P. (1984). Concentration of solar radiation by white backed photovoltaic panels. *Applied Optics*, *23*, 4394–4402.
- Su, Y., Pei, G., Riffat, S. B., & Huang, H. (2012). A novel lens-walled compound parabolic concentrator for photovoltaic applications. *Journal of solar energy engineering*, *134*(2), 021010.
- Sun, Y., Liu, X., Ming, Y., Liu, X., Mahon, D., Wilson, R., Liu, H., Eames, P., & Wu, Y. (2021). Energy and daylight performance of a smart window: Window integrated with thermotropic parallel slat-transparent insulation material. *Applied Energy*, *293*, 116826.
- Sun, Y., Shanks, K., Baig, H., Zhang, W., Hao, X., Li, Y., He, B., Wilson, R., Liu, H., Sundaram, S., Zhang, J., Xie, L., Mallick, T., & Wu, Y. (2018). Integrated semi-transparent cadmium telluride photovoltaic glazing into windows: Energy and daylight performance for different architecture designs. *Applied Energy*, *231*, 972–984.
- Sun, Y., Wilson, R., Liu, H., & Wu, Y. (2021). Numerical investigation of a smart window system with thermotropic parallel slat-transparent insulation material for building energy conservation and daylight autonomy. *Building and Environment*, *203*, 108048.
- Tällberg, R., Jelle, B. P., Loonen, R., Gao, T., & Hamdy, M. (2019). Comparison of the energy saving potential of adaptive and controllable smart windows: A state-of-the-art review and simulation studies of thermochromic, photochromic and electrochromic technologies. *Solar Energy Materials and Solar Cells*, *200*, 109828.
- Uematsu, T., Tsutsui, K., Yazawa, Y., Warabisako, T., Araki, I., Eguchi, Y., & Joge, T. (2003). Development of bifacial PV cells for new applications of flat-plate modules. *Solar Energy Materials and Solar Cells*, *75*, 557–566.
- Uematsu, T., Yazawa, Y., Joge, T., & Kokunai, S. (2001). Fabrication and characterization of a flat-plate static-concentrator photovoltaic module. *Solar Energy Materials and Solar Cells*, *67*, 425–434.
- Uematsu, T., Yazawa, Y., Tsutsui, K., Miyamura, Y., Ohtsuka, H., Warabisako, T., & Joge, T. (2001). Design and characterization of flat-plate static-concentrator photovoltaic modules. *Solar Energy Materials and Solar Cells*, *67*, 441–448.
- Unger, E., Kegelman, L., Suchan, K., Sörell, D., Korte, L., & Albrecht, S. (2017). Roadmap and roadblocks for the band gap tunability of metal halide perovskites. *Journal of Materials Chemistry A*, *5*, 11401–11409.
- Wang, M., Gao, Y., Cao, C., Chen, K., Wen, Y., Fang, D., Li, L., & Guo, X. (2014). Binary solvent colloids of thermosensitive poly (n-isopropylacrylamide) microgel for smart windows. *Industrial & Engineering Chemistry Research*, *53*, 18462–18472.
- Wang, M., Peng, J., Li, N., Lu, L., Ma, T., & Yang, H. (2016). Assessment of energy performance of semi-transparent PV insulating glass units using a validated simulation model. *Energy*, *112*, 538–548.
- Watanabe, H. (1998). Intelligent window using a hydrogel layer for energy efficiency. *Solar Energy Materials and Solar Cells*, *54*, 203–211.
- Watanabe, H. (2007). *Laminate-controlling light autonomously and window using the same*. Google Patents.
- Weber, K., Everett, V., Deenapanray, P., Franklin, E., & Blakers, A. (2006). Modeling of static concentrator modules incorporating lambertian or v-groove rear reflectors. *Solar Energy Materials and Solar Cells*, *90*, 1741–1749.
- Weber, K., Everett, V., Macdonald, J., Blakers, A. W., Deenapanray, P., & Babaei, J. (2004). *Modelling of silver modules incorporating a lambertian rear reflector*.
- Wheeler, L. M., Moore, D. T., Ihly, R., Stanton, N. J., Miller, E. M., Tenent, R. C., Blackburn, J. L., & Neale, N. R. (2017). Switchable photovoltaic windows enabled by reversible photothermal complex dissociation from methylammonium lead iodide. *Nature Communications*, *8*, 1722.
- Whole Building Design Guide. 2016. Window Film Fundamentals. Available: <https://www.wbdg.org/resources/window-film-fundamentals> [Accessed 15 June 2022].
- Wiegman, J., & Van Der Kolk, E. (2012). Building integrated thin film luminescent solar concentrators: Detailed efficiency characterization and light transport modelling. *Solar Energy Materials and Solar Cells*, *103*, 41–47.
- Wu, L. Y., Zhao, Q., Huang, H., & Lim, R. (2017). Sol-gel based photochromic coating for solar responsive smart window. *Surface and Coatings Technology*, *320*, 601–607.
- Wu, Y., Connelly, K., Liu, Y., Gu, X., Gao, Y., & Chen, G. Z. (2016). Smart solar concentrators for building integrated photovoltaic façades. *Solar Energy*, *133*, 111–118.
- Xia, X., Tang, S., Lu, X., & Hu, Z. (2003). Formation and volume phase transition of hydroxypropyl cellulose microgels in salt solution. *Macromolecules*, *36*, 3695–3698.
- Xu, S., Liao, W., Huang, J., & Kang, J. (2014). Optimal PV cell coverage ratio for semi-transparent photovoltaics on office building facades in Central China. *Energy and Buildings*, *77*, 130–138.
- Xue, Q., Xia, R., Brabec, C. J., & Yip, H.-L. (2018). Recent advances in semi-transparent polymer and perovskite solar cells for power generating window applications. *Energy & Environmental Science*, *11*, 1688–1709.
- Yamada, N., Kanno, K., Hayashi, K., & Tokimitsu, T. (2011). Performance of see-through prism CPV module for window integrated photovoltaics. *Optics Express*, *19*, A649–A656.
- Yang, Y.-S., Zhou, Y., Chiang, F. B. Y., & Long, Y. (2016). Temperature-responsive hydroxypropylcellulose based thermochromic material and its smart window application. *RSC Advances*, *6*, 61449–61453.
- Yao, J., & Yan, C.-W. (2010). Development and analysis of a novel kind of smart thermotropic material. *Functional Materials Letters*, *3*, 135–139.
- Yao, J., & Zhu, N. (2012). Evaluation of indoor thermal environmental, energy and daylighting performance of thermotropic windows. *Building and Environment*, *49*, 283–290.
- Yoshioka, K., Koizumi, K., & Saitoh, T. (2003). Simulation and fabrication of flat-plate concentrator modules. *Solar Energy Materials and Solar Cells*, *75*, 373–380.
- Yu, X., Su, Y., Zheng, H., & Riffat, S. (2014). A study on use of miniature dielectric compound parabolic concentrator (dCPC) for daylighting control application. *Building and Environment*, *74*, 75–85.
- Zacharopoulos, A., Eames, P. C., McLaren, D., & Norton, B. (2000). Linear dielectric non-imaging concentrating covers for PV integrated building facades. *Solar Energy*, *68*, 439–452.
- Zhang, Q., & Cao, G. (2011). Nanostructured photoelectrodes for dye-sensitized solar cells. *Nano Today*, *6*, 91–109.
- Zhang, Y., Sun, S., Kang, R., Zhang, J., Zhang, N., Yan, W., Xie, W., Ding, J., Bao, J., & Gao, C. (2015). Polymethylmethacrylate-based luminescent solar concentrators with bottom-mounted solar cells. *Energy Conversion and Management*, *95*, 187–192.
- Zhou, J., Gao, Y., Zhang, Z., Luo, H., Cao, C., Chen, Z., Dai, L., & Liu, X. (2013). VO₂ thermochromic smart window for energy savings and generation. *Scientific Reports*, *3*, 3029.
- Zhou, Y., Cai, Y., Hu, X., & Long, Y. (2014). Temperature-responsive hydrogel with ultra-large solar modulation and high luminous transmission for “smart window” applications. *Journal of Materials Chemistry A*, *2*, 13550–13555.
- Zhou, Y., Wang, S., Peng, J., Tan, Y., Li, C., Boey, F. Y. C., & Long, Y. (2020). Liquid thermo-responsive smart window derived from hydrogel. *Joule*, *4*, 2458–2474.
- Zhu, L., Shao, Z., Sun, Y., Soebarto, V., Gao, F., Zillante, G., & Zuo, J. (2018). Indoor daylight distribution in a room with integrated dynamic solar concentrating facade. *Energy and Buildings*, *158*, 1–13.

Publisher's Note

Springer Nature remains neutral with regard to jurisdictional claims in published maps and institutional affiliations.